UNIVERSIDADE DE SÃO PAULO
ESCOLA DE ENGENHARIA DE SÃO CARLOS

RIGOBERTO CASTRO CASTRO

Avaliação da Precisão de Sistema de Condução Autônoma baseada em GPS em um Veículo Agrícola por Métodos de Visão Computacional

São Carlos
2017

RIGOBERTO CASTRO CASTRO

Avaliação da Precisão de Sistema de Condução Autônoma baseada em GPS em um Veículo Agrícola por Métodos de Visão Computacional

Dissertação apresentada à Escola de Engenharia de São Carlos da Universidade de São Paulo, como requisito para a obtenção do Título de Mestre em Engenharia Mecânica.

Área de Concentração:
Dinâmica das Máquinas e Sistemas.

Orientadora: Dra. Maíra Martins da Silva
Co-orientador: Dr. Ricardo Yassushi Inamasu

ESTE EXEMPLAR TRATA-SE DA VERSÃO CORRIGIDA.
A VERSÃO ORIGINAL ENCONTRA-SE DISPONÍVEL JUNTO AO DEPARTAMENTO DE ENGENHARIA MECANICA DA EESC-USP.

EESC - USP
Biblioteca
CAMPUS DE S. CARLOS

São Carlos
2017

EESC/USP
Serviço de Pós Graduação
Protocolado em 07 / 12 / 2017

Class. TESE
Cutt. 9909

Tombo T283/17
Sysno 2864643
13.12.17

31100210603

AUTORIZO A REPRODUÇÃO TOTAL OU PARCIAL DESTE TRABALHO, POR QUALQUER MEIO CONVENCIONAL OU ELETRÔNICO, PARA FINS DE ESTUDO E PESQUISA, DESDE QUE CITADA A FONTE.

CC355a

Castro, Rigoberto
Avaliação da Precisão de Sistema de Condução Autônoma baseada em GPS em um Veículo Agrícola por Métodos de Visão Computacional / Rigoberto Castro; orientadora Maira Martins da Silva; coorientador Ricardo Inamasu. São Carlos, 2017.

Dissertação (Mestrado) - Programa de Pós-Graduação em Engenharia Mecânica e Área de Concentração em Dinâmica das Máquinas e Sistemas -- Escola de Engenharia de São Carlos da Universidade de São Paulo, 2017.

1. Visão computacional. 2. Processamento de imagem. 3. Navegação GPS RTK. 4. Veículos inteligentes. 5. Agricultura de precisão. I. Título.

FOLHA DE JULGAMENTO

Candidato: Engenheiro **RIGOBERTO CASTRO CASTRO**.

Título da dissertação: "Avaliação da precisão de um sistema de navegação autônoma baseado em um sistema de posicionamento global de um veículo agrícola por método de visão computacional".

Data da defesa: 21/11/2017.

Comissão Julgadora:	**Resultado**:
Profa. Dra. **Maíra Martins da Silva** **(Orientadora)** (Escola de Engenharia de São Carlos/EESC)	APROVADO
Prof. Dr. **Rubens André Tabile** (Faculdade de Zootecnia e Engenharia de Alimentos/FZEA-USP)	REPROVADO
Prof. Dr. **André Camona Hernandez** (Universidade Federal de São Carlos/UFSCar)	APROVADO

Coordenador do Programa de Pós-Graduação em Engenheira Mecânica:
Prof. Associado **Gherhardt Ribatski**

Presidente da Comissão de Pós-Graduação:
Prof. Associado **Luís Fernando Costa Alberto**

Dedicated to my mother for being my
main motivation, my family for the
tireless support at every phase of my life.
To my grandmother for being the
greatest example of love and sacrifice.

ACKNOWLEDGMENTS

To God for always being with me and never let me down.

To my mother Camila Castro for being my main motivation.

To my sisters Cintya, Diana, Faviola and my niece Camila for always supporting me.

To my family for support in these difficult years away from home.

To my friends who encouraged me in all these years.

To Dr. Maira Martins da Silva, for her unconditional support during my professional growth to achieve this goal.

To Dr. Ricardo Yassushi Inamasu for the confidence and the opportunity to work together on the Embrapa research.

To Dr. Ladislau Marcelino Rabello for his unconditional help for the realization of this research.

To CAPES Foundation for the financial support for this research.

To Lanapre technical personnel for their assistance to achieve this research.

To all my postgraduate teachers of EESC for the teachings and advice during my academic master's degree education.

To Embrapa for the great opportunity to work on this research.

“Have I not commanded you? Be strong and courageous. Do not be afraid; do not be discouraged, for the LORD your God will be with you wherever you go.”
Joshua 1:9

RESUMO

CASTRO, R. C. **Avaliação da precisão de um sistema de condução autônoma baseada em GPS em um veículo agrícola por métodos de visão computacional.** 2017. 74 f. Tese (Mestrado) – Escola de Engenharia de São Carlos, Universidade de São Paulo, São Carlos, 2016.

Avanços tecnológicos foram alcançados com sucesso na agricultura de precisão utilizando sistemas de condução autônoma em veículos agrícolas. Entre esses avanços, destaca-se o aumento da eficiência e da produtividade nas operações de campo. Alguns sistemas de condução autônoma são implementados usando o sistema GPS RTK, que permite operações com precisão centrimétrica. No entanto, os erros de posicionamento geográfico, a dinâmica do veículo, os implementos agrícolas e ambiente de campo (encostas, condições do solo, etc.) podem influenciar o desempenho dos veículos agrícolas autônomos. Desta forma, a avaliação dos sistemas de condução autônoma torna-se essencial para a obtenção de altos níveis precisão. Esta avaliação pode ser realizada medindo os deslocamentos usando sensores instalados no veículo, tais como: câmeras, lasers, odômetro, sensores ultrassônicos, entre outros. Entre as opções, o método de visão computacional permite a localização de qualquer sistema no espaço, tornando-se uma alternativa técnica para esta avaliação. Desta forma, o objetivo desta pesquisa é propor um método para a avaliação da precisão dos sistemas de auto-orientação em condições reais de operação usando métodos de visão computacional. O veículo em estudo é um trator equipado com um sistema de auto-orientação o qual é integrado por uma unidade GPS RTK e por uma unidade de medição inercial (IMU). A instrumentação utilizada no desenvolvimento do sistema de visão computacional consiste em duas câmeras Canon Rebel T5 com lente focal de 50 e 18 milímetros, respectivamente. Foi utilizado o método de câmera pinhole para mapear a localização do veículo no campo usando técnicas de visão computacional. No estudo foram realizados múltiplos testes de campo, provando assim que o uso do método de visão computacional é preciso para avaliar sistemas de auto-orientação se dispositivos, procedimentos e parâmetros forem selecionados corretamente.

Palavras-chave: Visão computacional. Processamento de imagem. Navegação GPS RTK. Veículos inteligentes. Agricultura de precisão.

ABSTRACT

CASTRO, R. C. **Precision Evaluation of a GPS based auto-guidance system in an agricultural vehicle by computational vision methods**. 2017. 74 p. MSc. Thesis, São Carlos School of Engineering – University of São Paulo, São Carlos, 2017.

Technological advances have been successfully achieved in precision agriculture using auto-guidance systems in agricultural vehicles. Among these advances, the increase of efficiency and the productivity in field operations can be highlighted. Some auto-guidance driving systems are implemented using the GPS RTK system, which allows operations to centimeter accuracy. However, the geographic positioning errors, the vehicle dynamics, the agricultural devices and the field environment (slopes, soil condition, etc.) may influence the performance of GPS based autonomous agricultural vehicles. In this way, the evaluation of the auto-guidance driving systems becomes essential to the achievement of high precision levels in field operations. This evaluation can be performed by measuring the displacements using precise sensors installed in the vehicle, such as: cameras, lasers, odometer, and ultrasonic sensors, among others. Among the local sensing options, it is well-know that computational vision methods allow the location of any system in the space, becoming it a technical alternative for this evaluation. In this way, the objective of this research is to propose a methodology to assess the accuracy of auto-guidance systems under real field conditions.by means of computer vision methods. The vehicle under study is a tractor equipped with an auto-guidance system, which is composed of a GPS RTK unit and an inertial measurement unit (IMU). The instrumentation consisted of two Canon Rebel T5 cameras with focal lens of 50 and 18 millimeters respectively. The pinhole camera method was used to map vehicle location in the field using computational vision techniques. In the study, multiple field tests were performed, proving that the use of the computer vision method is accurate to evaluate auto-guidance systems if devices, procedures, and parameters are properly selected.

Keywords: Computational vision. Image processing. RTK GPS Navigation. Smart vehicles. Precision agriculture.

LIST OF FIGURES

Figure 1 – Visual sensor auto-guidance testing system 10
Figure 2 – Intellect software interface locating a segment of tracked line 11
Figure 3 – Test laboratory track for the research 12
Figure 4 – The fundamental steps in digital image processing 15
Figure 5 – Recognition by patterns 17
Figure 6 – Types of flowers described by two descriptors 18
Figure 7 – Planar checkerboard pattern 19
Figure 8 – Checkerboard pattern detection by internal corners using the single camera calibration application (Matlab) 20
Figure 9 – The arrangement of internal corners and the origin point 21
Figure 10 – Results and errors of calibration 21
Figure 11 – Computational time cost 22
Figure 12 – Stages of stereo system construction 22
Figure 13 – Epipolar geometry 24
Figure 14 – Stereo system in standard form 24
Figure 15 – Stereo images in standard form with cameras correctly aligned 25
Figure 16 – Geometry of a stereo system 25
Figure 17 – Disparity and depth in stereo vision 26
Figure 18 – Disparity map in stereo vision 27
Figure 19 – Baseline between camera lenses 27
Figure 20 – Parallel planes with minimum and maximum distances of perception 28
Figure 21 – 2-D space to 3-D space conversion 29
Figure 22 – Camera location mapping 30
Figure 23 – Camera location mapping process 30
Figure 24 – Extrinsic parameters of the camera 31
Figure 25 – Skew coefficient 32
Figure 26 – Types of radial distortions of lenses 32
Figure 27 – Tangential distortion of lenses 33
Figure 28 – System coordinates applied in the efficiency evaluation 34
Figure 29 – Comparison and contrasting of location data of both systems 37

Figure 30 – Examples of stereo pairs loaded into the stereo camera calibration application (Matlab)........ 40
Figure 31 – Accuracy error vs baseline at 10 meters........ 41
Figure 32 – Accuracy error vs baseline at 15 meters........ 41
Figure 33 – Accuracy error vs baseline at 20 meters........ 42
Figure 34 – Accuracy error vs baseline at 25 meters........ 42
Figure 35 – Pinhole camera model........ 43
Figure 36 – Arrangement positioning for accuracy test........ 44
Figure 37 – Set of images for the accuracy test (Camera pinhole method)........ 45
Figure 38 – Single camera mounted on the test tractor........ 46
Figure 39 – Single camera mounted on the rear of the tractor........ 46
Figure 40 – Desired programmed path and error of auto-guidance system........ 48
Figure 41 – The checkerboard pattern on the field at LANAPRE – Embrapa Instrumentation São Carlos........ 49
Figure 42 – Camera vertically located at the rear of the tractor (validation test)........ 50
Figure 43 – Detection of rope on the paved surface. A) Original image B) Processed image 51
Figure 44 – Checkerboard pattern using to calibrate the vertical located camera........ 51
Figure 45 – Accuracy tests with stereo vision method until 10 meters........ 53
Figure 46 – Location mapping of calibration images for the pinhole camera method until 25 meters........ 55
Figure 47 – Planar checkerboard pattern detection in field test........ 56
Figure 48 – Mapping of tractor trajectory in auto-guidance mode at 4.0 km/h........ 56
Figure 49 – Mapping of tractor trajectory in auto-guidance mode at 4.5 km/h........ 57
Figure 50 – Mapping of tractor trajectory in auto-guidance mode at 5.0 km/h........ 57
Figure 51 – Mapping of tractor trajectory in auto-guidance mode at 5.5 km/h........ 58
Figure 52 – Auto-guidance system error at 4.0 km/h........ 58
Figure 53 – Auto-guidance system error at 4.5 km/h........ 59
Figure 54 – Auto-guidance system error at 5.0 km/h........ 59
Figure 55 – Auto-guidance system error at 5.5 km/h........ 60
Figure 56 – Auto-guidance system errors, validation method vs pinhole camera method (4.0 km/h)........ 63
Figure 57 – Auto-guidance system errors, validation method vs pinhole camera method (4.5 km/h)........ 63

Figure 58 – Auto-guidance system errors, validation method vs pinhole camera method (5.0 km/h) 64
Figure 59 – Auto-guidance system errors, validation method vs pinhole camera method (5.5 km/h) 64

LIST OF TABLES

Table 1 – Stereo system specifications 39
Table 2 – Camera pinhole method specifications 44
Table 3 – Auto-guidance system specifications 47
Table 4 – Field test specifications 49
Table 5 – Accuracy of pinhole camera method at different distances 54
Table 6 – Number of frames processed at each operating speed 55
Table 7 – Auto-guidance system errors 60
Table 8 – Number of frames processed using the validation methodology 61
Table 9 – Auto-guidance system errors using the validation methodology 61
Table 10 – Auto-guidance system errors using the pinhole camera method on flat surface 62
Table 11 – Auto-guidance system errors using validation methodology vs pinhole camera method 62

LIST OF ABBREVIATIONS AND ACRONYMS

2-D	Two dimension
3-D	Three dimension
AI	Artificial intelligence
Anfavea	National Association of Motor Vehicle Fabricators (Brazil)
ESALQ-USP	Escola Superior de Agricultura Luiz de Queiroz – Universidade de São Paulo
EVI	Enhanced vegetation index
GNSS	Global navigation satellite system
GOSAVI	Green optimized soil adjusted vegetation index
GPS	Global positioning system
GSAVI	Green soil adjusted vegetation index
IMU	Inertial Measurement Unit
INS	Inertial navigation system
NDVI	Normalized difference vegetation index
OSAVI	Optimized soil-adjusted vegetation index
PA	Precision agriculture
RTK	Real time kinematic
SAVI	Soil-adjusted vegetation index
SVI	Simple vegetation index
UIF	Unscented Information Filter
UTM	Universal Transverse Mercator

LIST OF SYMBOLS

LATIN SMALL LETTERS

$[c_x \; c_y]$	Optical center in pixels
d_{max}	Maximum disparity
d_{min}	Minimum disparity
$[f_x \; f_y]$	Focal length in pixels
$[ox_n \; oy_n]$	Location of the optical center of the vision system
$[p_x \; p_y]$	Pixel size in measurement system (typically measured in mm)
q_1, q_2	Tangential distortion coefficients
w	Scale factor
$[x, y]$	Image point

LATIN CAPITAL LETTERS

B	Baseline, linear distance between camera lenses
ε_{SV}	Average error in stereo vision
ε_X	Percent accuracy error in x coordinate
ε_Y	Percent accuracy error in y coordinate
ε_Z	Percent accuracy error in z coordinate
F	Focal length of camera (measured in mm)
K	Matrix of intrinsic parameters
P	Camera matrix
R	Rotation
S	Skew coefficient
T	Translation
T_{yn}	Translation in y-coordinate at n-th frame
T_{zn}	Translation in z-coordinate at n-th frame
$V_L (X_L, Y_L, Z_L)$	Vehicle location vector with respect to the checkerboard
X	Location X coordinate
X'	Coordinate x determined by software from vision system to checkerboard

X_R	Lateral distance of object in perception in the reference image (Measured in pixels)
X_T	Lateral distance of object in perception in the target image (Measured in pixels)
Y	Location Y coordinate
Y'	Coordinate y determined by software from vision system to checkerboard
Y_R	Vertical distance in object pixels in perception in the reference image
Y_R	Vertical distance in object pixels in perception in the reference image
$[X_{Dis}\ Y_{Dis}]$	Distorted points on images
Z	Location Z coordinate
Z'	Coordinate Z determined by software from vision system to checkerboard

GREEK SMALL LETTERS

δ	Descriptor of an object in a digital image
η_{2D}	Planar efficiency
η_{3D}	Stereo efficiency
θ	Rotation angle on the XY plane
ρ	Pattern of an object in a digital image

SUMMARY

1 INTRODUCTION 1

1.1 Objective 3

1.2 Text organization 4

2 LITERATURE REVIEW 7

2.1 Methodologies for location mapping using computational vision 8

2.1.1 Stereo vision method 8

2.1.2 Pinhole camera method 9

2.2 Evaluation of auto-guidance system by computational vision methods 10

3 METHODOLOGY 13

3.1 Image processing 13

3.2 Recognition and location of internal corners of planar checkerboard pattern 18

3.2.1 Procedure to recognize a checkerboard pattern using Matlab 20

3.2.2 Location of the internal corners of checkerboard pattern 20

3.3 Stereo vision method 22

3.3.1 Stereo geometry 23

3.3.2 Map of disparity and depth 25

3.3.3 Calculating 3-D coordinates 28

3.4 Pinhole camera method 29

3.4.1 Calibration parameters 30

3.4.2 Extrinsic parameters 30

3.4.3 Intrinsic parameters 31

3.4.4 Distortion in camera 32

3.5 Evaluation of visual systems 34

3.6 Evaluation of auto-guidance system 35

4 DESCRIPTION OF EXPERIMENTS 39

4.1 Modeling of visual systems 39

4.1.1 Stereo vision method modeling 39

4.1.2 Pinhole camera method modeling 43

4.2 Mapping of tractor position in the field 45

4.3 Specifications of the tractor and auto-guidance system tested 47

4.4 Test procedure development 47
4.5 Validation of methodology 50
5 RESULTS AND DISCUSSION 53
5.1 Accuracy evaluation Stereo Vision Method - Camera Pinhole Method 53
5.1.1 Stereo vision method 53
5.1.2 Pinhole camera method 54
5.2 Evaluation of the auto-guidance system on ground surface 55
5.3 Validation of methodology 61
6 CONCLUSIONS 67
6.1 Future perspectives 68
BIBLIOGRAPHIC REFERENCES 69

1 INTRODUCTION

The emergence of precision agriculture (PA) has bringing technological advances in the modernization of production practices by means of the use of sensors, actuators, and control techniques. PA techniques have been explored since the 80's. At that time, the first map of productivity was elaborated in Europe using sensors and data acquisition techniques, and the first fertilizer with varied doses was used in the field using control techniques in the USA (MINISTERIO DA AGRICULTURA, PECUÁRIA E ABASTECIMENTO, 2009). The true advances in PA were achieved with the exploitation of Global Positioning System (GPS) satellite signals. In fact, the installation of receivers into harvesters enable the storage of instantaneous production data. The first Global Navigation Satellite System (GNSS) was proposed in the USA in 1978 and the system became commercially available in the 90´s.

In Brazil, the use of PA began in 1995 when agricultural machinery equipped with productivity monitors were imported. Researches on PA were launched in 1996 during the first Symposium on PA held at ESALQ-USP (BALASTREIRE, 2000). In 1999, the program Moderfrota promoted the introduction of modern technologies in agricultural machinery. Since then, the Brazilian agriculture has had enormous benefits in the area of sustainability and quality by means of PA.

There are multiple techniques of computer vision that can be applied in the agricultural field, which has encouraged the development of several utilities in PA. In fact, image processing in PA has become essential. Among the main applications of image processing in PA, the following ones can be mentioned:

1. Remote sensing systems: is the most used application in PA. Aerial images of crops taken by drones may provide important information about the field. By implementing the appropriate image processing techniques, relevant information of productivity can be extracted. This technique can be also exploited to generate crop maps aiding its management.

2. Diagnosis of planting lines: leaf pigmentation in plants may reveal important information. In fact, the chlorophyll is a strong radiation absorber in visible spectra (400 to 700 nm), and, plants are highly reflective near infrared (700 to 1300 nm) (BRANDÃO *et al.*, 2008). Using image processing techniques, the health conditions of plants can be assumed by monitoring the color of their leaves.

3. Vegetation indexes: with crop images and image processing techniques, different indices can be designed to determine the green patch of a land and analyze the vegetation properties. Among them, NDVI (Normalized Difference Vegetation Index), SVI (Simple Vegetation Index) and EVI (Enhanced Vegetation Index) are commonly used for the vegetation classification. A variety of indexes have also been proposed for analyzing soil parameters, among them, it can be mentioned: SAVI (Soil-Adjusted Vegetation Index), GSAVI (Green Soil Adjusted Vegetation Index), OSAVI (Optimized Soil-Adjusted Vegetation Index), and GOSAVI (Green Optimized Soil Adjusted Vegetation Index).

4. Auto-guidance systems in agricultural vehicles: vehicles with auto-guidance systems are assisted by GPS systems to carry out operations in the crop areas. In addition, many vehicles integrate the GPS system with optical systems to perform the control correction of the auto-guidance systems implementing different techniques of image processing in real time.

Nowadays, the GPS is widely used in agricultural vehicles, being employed in the implementation of auto-guidance driving systems (also called auto-steering systems). The auto-guidance driving systems present great advantages in agricultural production, among them: the increase of working hours per machine, the greater amount of worked areas, the reduction of the machine's maintenance and the increase of the machine speed. In fact, auto-guidance systems allow a greater control of operations in the field, a reduction of passes of the vehicle through the terrain than expected, thereby reducing soil compaction.

Most of auto-guidance driving systems allow precise operations. However, the geographic positioning errors, the vehicle dynamics, the agricultural equipment and the field environment (slopes, soil condition, etc.) may influence the accuracy of GPS based autonomous agricultural vehicles. In this way, the agricultural vehicles are subjected to undesired errors. Consequently, several methods have been proposed to reduce them.

The precision of the position data derived from satellite-based positioning systems, such as GPS, can be improved by means of Real Time Kinematic (RTK) satellite navigation. This methodology is capable of providing real-time corrections since it does not only rely on the satellite signals but also on the data content of the measurements (phase, interpolations, prediction, etc.). Due to the use of these techniques, GPS RTK technology allows centimeter-level accuracy. Nevertheless, the accuracy and robustness of this technology should be assessed during field operations.

During field operation, the auto-guidance systems may present errors. Therefore, in order to guarantee a satisfactory field coverage, the number of passes of the vehicle in a field should be increased. However, the more the number of passes of the vehicle over an area, the less economic efficiency is the agricultural operation. This fact considerably increases the costs these operations. For that reason, the precision of auto-guidance systems has a great impact on the optimization of field operations and their economic efficiency.

1.1 Objective

The agricultural vehicle under evaluation is equipped with a commercial auto-guidance system assisted by a GPS RTK unit and an inertial measurement unit (IMU). The field operations can be programmed and automatically executed using the auto-guidance system. According to its technical specifications, this system has centimeter-level accuracy. However, it is well know that field environment conditions (such as slopes, soil condition, etc.), the vehicle dynamics, the agricultural equipment, among other issues may influence the accuracy of the auto-guidance system installed in the agricultural vehicle. It is a fact that each crop area has its own characteristics and conditions. Therefore, the auto-guidance system has a certain accuracy for those conditions of the terrain. In this way, the assessment of the accuracy of this auto-guidance system under particular conditions may aid the user/designer to infer about the auto-guidance system accuracy in a specific crop area.

The main objective of this work is to propose a methodology to assess the accuracy of auto-guidance systems under real field conditions. This presents an important advance in precision agriculture, as there is currently no standard procedure for assessing the accuracy of auto-guidance systems under specific field conditions. In this research, the accuracy of an auto-guidance system installed on a tractor was evaluated using computational vision. This evaluation was performed by tracking the localization of the vehicle using the extrinsic visual method while the vehicle advanced on a straight line programmed by the auto-guidance system. This extrinsic visual method was implemented by means of a local visual sensing equipment and image processing techniques to map the localization of the vehicle in the field.

Two cameras Canon Rebel T5 with focal lens of 18 millimeters were mounted on the rear side of the tractor. These cameras were used to take several digital images of a checkerboard placed on a fixed position on the working field at LANAPRE - Embrapa Instrumentation São Carlos. These digital images were processed to identify the features of the checkerboard pattern and calculate the parameters of the computational visual system. Using the parameters of the visual system it was possible to track the location of the vehicle in the field at each image. In this work, two computational visual systems were initially evaluated: the stereo vision method and the camera pinhole method.

The following objectives of this research can be described:

1. The proposal of a strategy based on local visual sensing equipment and image processing techniques for measuring the localization of an agricultural vehicle in the working field.
2. The comparison between two computational vision techniques: the stereo vision method and the camera pinhole method, for assessing the vehicle's localization.
3. The assessment of the localization of the vehicle during the execution of an autonomous motion (a straight-line trajectory).
4. The evaluation of the auto-guidance system at field operations velocities using as metrics the average and maximum errors.
5. The validation of the proposed methodology using the comparison with a proved and established procedure using computational vision.

1.2 Text organization

The text has been organized as follows:

Chapter 2. This chapter presents the required theoretical background to develop this research. In this chapter, the methods to map the position of vehicles in outdoor environments, and the developed researches to evaluate the auto-guidance systems using image processing are described.

Chapter 3. This chapter presents a short review of the basic concepts of image processing. This chapter also presents the important design patterns and software tools used for the construction of the stereo vision method and pinhole camera method evaluated in this research. In addition, this chapter presents a detailed explanation of the methodology proposed in this work to evaluate auto-guidance systems using computational vision.

Chapter 4. This chapter describes the tests to evaluate the accuracy of the visual systems compared in this research (stereo vision method/ pinhole camera method). In addition, this chapter explains the tests development in the field and the experimental procedure to evaluate the feasibility and quality of the proposal.

Chapter 5. The results are presented and discussed in this chapter.

Chapter 6. Conclusions and future perspectives are presented in this chapter.

2 LITERATURE REVIEW

The self-management systems encourage an increase in the capacity to cultivate more areas with the same machinery because of the increase in hours worked, greater speed of operation and reduction of vehicle passes. The precision of self-management systems installed in agricultural vehicles is greatly related to the precision of the GPS components mounted on the machinery. The assessment of GPS errors in agricultural vehicles has been the subject of several research papers. It can be performed by measuring the displacements in outdoor environment using precise sensors installed in the vehicle, such as: cameras, lasers, odometer, and ultrasonic sensors.

There have been multiple research in which the accuracy of GPS systems installed in different mobile vehicles were evaluated in outdoor environment. Yang and Farrell (2013) used a triple redundancy navigation system incorporating a magnetometer, inertial navigation system (INS), and a carrier phase differential GPS to accurately estimate vehicle latitude (including yaw). The system was designed to operate in any weather condition and work even in the absence of the GPS. The navigation system provides vehicle position, velocity, acceleration, pitch and roll, yaw, and angular rates. Liu *et al.* (2005) developed a multi-aided inertial based localization system using odometry, an accurate gyroscope, and vehicle constraints. This system is capable of finding the localization of an autonomous vehicle in the field. Cui and Xu (2007) developed a method integrating GPS, INS and odometer data using a Kalman filter to compensate the errors of navigation in a moving vehicle in the field.

Among the local sensing options, it is well known that computer vision methods allow the location of any system in the space. Advances in computational capacity improve the effectiveness of image processing methods increasing the accuracy of computational calculations and reducing processing time. In this way, the use of image processing techniques in PA has steadily increased. Rovira-Más *et al.* (2005) implemented a stereo camera and image processing techniques to identify planting lines. The authors proposed a control strategy for the auto-guidance system using the identification of the plating lines. Chon *et al.* (2011) and Wei *et al.* (2011) proposed the integration algorithms for using data obtained from different sensors. Chon *et al.* (2011) used data obtained from a stereo camera, a GPS and an INS to locate the vehicle in the field. On the other hand, Wei *et al.* (2011) used data from a stereo camera, a laser locator and a GPS to calculate the location of a vehicle in the field.

Some authors, as Easterly *et al.* (2010) and Harbuck *et al.* (2006) were able to improve considerably the accuracy of the GPS RTK to millimeter-level using computer vision techniques. Easterly *et al.* (2010) used a vision sensing method to measure the trajectory errors of a tractor with auto-guidance system. In this research, an optical vision sensor was rigidly mounted at the rear of the tractor. The vision sensor measured a location of a reference line on the paved surface located at the center of the drawbar. The deviation of the tractor's actual travel path from its desired path could be assessed from the measurement of the reference line. Harbuck *et al.* (2006) assess different auto-guidance systems, using from WAAS to RTK differential correction, over various periods. A non-GPS-based surveying practice was used to establish the absolute equipment traverse during testing. This information was then used to compute path deviations from the desired traverse. In each test, the tractor was operated using the auto-guidance system, and the relative position of the vehicle was continuously recorded. The 5 mm measurement error of the total station was applicable under ideal conditions, but this error increased to 20 mm during the test. Consequently, the order of magnitude required for greater accuracy by the measurement method was no longer valid.

This chapter presents a summary of the main methodologies used to track the location of vehicles at outdoor environments and a review of the previous researches done to evaluate auto-guidance systems using computer vision.

2.1 Methodologies for location mapping using computational vision

2.1.1 Stereo vision method

Stereo vision is an important technique in computer vision. This technique allows the calculations of the 3-D coordinates of objects in a field view by means of two aligned cameras. The method consists of aligning horizontally two cameras and the difference between the views produce a 3-D coordinate map. The idea of this method is based on how the human vision perceives the location of objects in a field view. In spite of being a cheap method, it has a high computational cost since it requires the implementation of a considerable set of computational vision processes. This is a common method in many fields of technology, such as robotics (ROVIRA-MÁS, WANG and ZHANG, 2009). In fact, a mobile robot must have accurate information about the surrounding environment in order to operate safely. This method is used in agricultural vehicles for correction of autonomous driving systems by digital images captured in real time. Rovira-Más *et al.* (2005) used a stereo system and computer vision methods for the detection and location of planting lines to perform the correction of auto-guidance systems in real time. Chon *et al.* (2011) developed a vehicle location algorithm by stereo vision system integrated to a GPS/INS system. The stereo system improved the location data of the vehicle in an open environment, since GPS/INS system do not guarantee accuracy and robustness of localization due to their vulnerability to external disturbances. Wei *et al.* (2011) used an Unscented Information Filter (UIF) to integrate information acquired from a stereo vision system, a laser range finder and a GPS receiver in order to provide robust vehicle localization results. Section 3.3 presents the theoretical and mathematical fundamentals for the technical design of the stereo system developed in this work.

2.1.2 Pinhole camera method

The pinhole camera is implemented using a simple camera with no optical lenses and a narrow viewing angle. The rays of light pass through the viewing angle and project an inverted image on the opposite side of the camera, capturing an inverted image of the scene. By knowing the parameters of the lens of the camera and of its optical sensor, the size of objects in an image and the location of the camera in the scene can be calculated. The method defines geometric relationships between a 3-D point and its corresponding 2-D point on the plane of the image scene. This mapping process from 3-D to 2-D is called perspective projection. This data is used for the detection and measurement of objects in digital images. The pinhole camera method is used in robotics for navigation systems and reconstruction of 3-D scenes. Royer *et al.* (2007) presented a real-time localization system for a mobile robot. The research showed that navigation in outdoor environment is possible using the pinhole camera method and natural landmarks. To do that, a three-step approach was developed. In the first step, the robot was manually guided on a path and a video record the sequence. Then, a motion algorithm was used to build a 3-D map of this path. Finally, the robot used the map to compute its location in real-time. Lin (2012) developed an algorithm that detects and tracks moving objects with a single camera. The camera parameters were estimated using the camera pinhole method. Features of points in a sequence of images captured by the camera were grouped using a hierarchical clustering algorithm. Then, the related groups between adjacent frames are linked and the sequence built a 3-D map. Experimental tests showed that the method presents an excellent performance to detect and track objects, and performed perfectly in complex environments. Cherubini *et al.*, (2013) designed and validated an approach that detects obstacles in the vicinity of a wheeled vehicle to achieve safe visual navigation in outdoor environments. The vehicle was guided by the camera pinhole method and a lidar, the vehicle followed a path represented by key images, avoiding collisions with the obstacles. Section 3.4 presents the theoretical and mathematical fundamentals for the technical design of the pinhole camera method to map the localization of the vehicle in this research. The construction of the visual system is based in the model developed by Bouguet (2004).

2.2 Evaluation of auto-guidance system by computational vision methods

An interesting and practical approach to evaluate auto-guidance systems was proposed by Easterly and Adamchuck (2008). This approach used a visual sensor mounted on the tractor to visualize the lateral displacements of the vehicle in auto-guidance mode. The programmed trajectory was a straight line. To test the performance of an agricultural tractor equipped with an auto-guidance system, one visual sensor was fixed to the chassis on the rear of the tractor. This sensor was mounted on the central line approximately 1.5 m above the ground and was positioned directly downward. This scheme allowed less than 2 mm resolution for the acquired image. Figure 1 shows the position of the optical sensor mounted to the chassis of the tractor with the lens pointed to the downward so that the field of view was centered on the drawbar hitch pivoting location.

Figure 1 – Visual sensor auto-guidance testing system

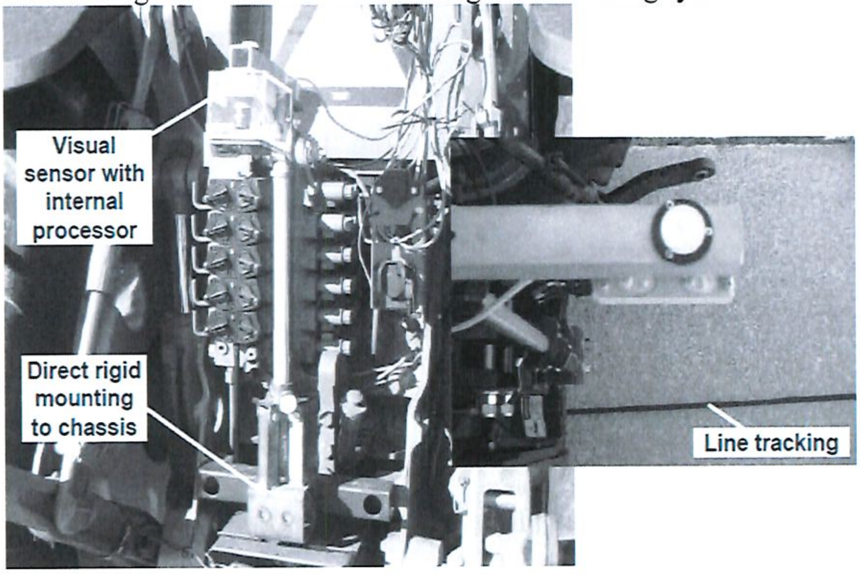
Visual sensor with internal processor
Direct rigid mounting to chassis
Line tracking

Source – Easterly *et al.* (2010)

Once the sensor was calibrated, by means of computer vision methods, it was possible to identify the parallel line to the direction of the programmed travel path and to determine its horizontal offset coordinate with respect to the central reference position of the tractor. With this approach, it was possible measure the lateral displacement of the real travel path made by the auto-guidance system with respect to the programed path (EASTERLY and ADAMCHUCK, 2008). Figure 2 shows the identification of the line using Intellect software.

The developed test procedure was based on a typical field of operation in which a series of back and forth parallel passes across a certain distance were performed by the tractor in auto-guidance mode. At the end of each pass, the vehicle was turned around and returned on a path adjacent to the previous pass. The track consisted of two east-west oriented straight passes 39.9 m (131 ft) apart from each other. Both passes were equal, and the total length of the central line around the track was approximately 600 m. Only the northern and southern straight passes of the track were used to measure auto-guidance system error. During tests, the tractor operated on auto-guidance mode during its passage through the straight sections. Figure 3 shows the test track used.

Figure 2 – Intellect software interface locating a segment of tracked line

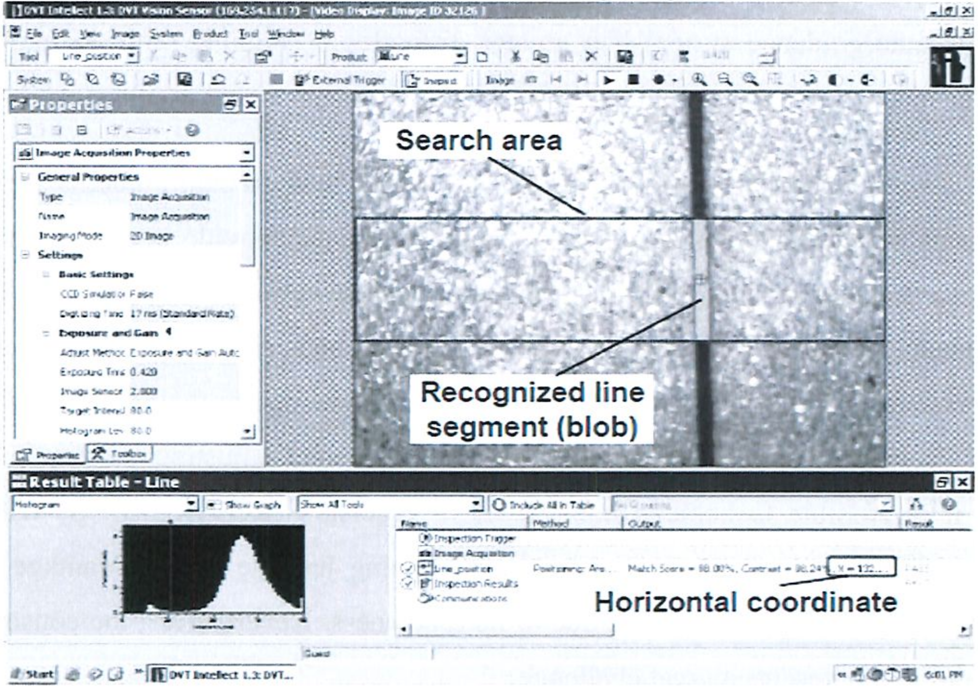

Properties
Image Acquisition Properties
General Properties
Settings
Basic Settings
Exposure and Gain
Properties
Toolbox
Result Table - Line
Histogram
Show Graph
Show All Tools
Search area
Recognized line segment (blob)
Horizontal coordinate

Type Image Acquisition
Name Image Acquisition
Imaging Mode 2D Image
CCD Simulator False
Digitizing Time 17 ms (Standard Rate)
Adjust Method Exposure and Gain Auto
Exposure Time 0.420
Image Sensor 2.000
Target Intensity 80.0
Histogram Lev 80.0

Source – Easterly *et al.* (2010)

Figure 3 – Test laboratory track for the research

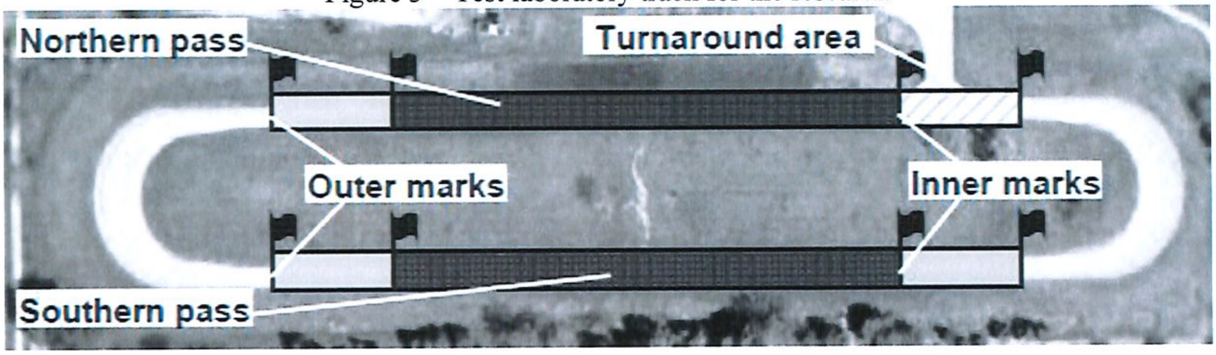

Source – Easterly *et al.* (2010)

The position of the tractor was detected for repeated passes; the track error was calculated as the difference between the desired path on the lines in the straight sections and the actual path performed by the auto-guidance system. The tractor traveled at speeds ranging from 0.5 m/s to 5.0 m/s. It was shown that relatively high travel speed (5 m/s) resulted in a substantially higher auto-guidance error as compared to the two slower speeds (1 and 2.5 m/s). For the slow and medium speeds, 95% values of errors were found comparable to the claims published in the literature (less than 2.5 cm). It was concluded that, for high operating speeds (5 m/s), the auto-guidance system had greater difficulty in aligning with the programmed operating line.

Visual systems for location mapping of vehicles in open environments are typically used in combination with other geo-referencing systems to provide accurate data. Visual systems are currently used in integration with auto-guidance systems in agricultural vehicles to correct the auto-guidance system on real-time (ROVIRA-MÁS *et al.*, 2005). However, they are less used to evaluate the precision of auto-guidance systems due to their lack of precision at millimeter level. However, by building a visual system and adjusting the test parameters correctly, it is possible to achieve high levels of precision (ROVIRA-MÁS, WANG and ZHANG, 2008). A visual system for location mapping has the great advantage of being applicable in variable field conditions due to its robustness. Nevertheless, the construction of the methodology represents a great challenge.

3 METHODOLOGY

The methodology proposed in this work exploits the use of computational vision to evaluate the auto-guidance systems. This is performed by mapping the position of the vehicle in the field. Therefore, a summary of the most important concepts of computational vision is presented hereafter. This research explores two computational vision techniques to map the location of a vehicle in outdoor environments. Based on their accuracy and adequacy, one of them is selected for accomplishing the research objectives. These techniques are the stereo vision method and the pinhole camera method. Firstly, the procedure to identify and localize a checkerboard pattern through image processing is presented. This procedure is of vital importance for the calibration of the visual systems. Moreover, this chapter also presents a review of the most important design patterns and software tools to develop the stereo camera method and camera pinhole method.

The Computer Vision System Toolbox is available in Matlab and is exploited in this research. This toolbox is used: (1) to detect the pattern of a checkerboard, (2) to perform the calibration of the stereo camera method and the pinhole camera method and (3) to locate the position of the checkerboard in a 3D environment. Details about the available techniques are described hereafter.

This chapter is divided into 6 sections. Section 3.1 presents a summary of the most important concepts of computational vision. Section 3.2 presents the methodology to recognize and to locate a planar checkerboard pattern in the field. Sections 3.3 and 3.4 summarize the stereo camera method modeling and the pinhole camera method modeling for this research, respectively. Section 3.5 presents the methodology to evaluate the accuracy of visual systems for 3-D location mapping. Section 3.6 presents the methodology that serves as a validation procedure of the proposal presented in this paper.

3.1 Image processing

Image processing is the set of operations that can be applied to digital images. It is important to note that a digital image is a set of finite values of elements with coordinates *x, y,* and an intensity. These elements are defined as pixels (GONZALEZ and WOODS, 2008).

Many of the current applications of image processing are operations based on the information obtained from the image. These operations can be the classification of groups of pixels, the detection of an object, the encoding of characters, among other functions that humans intuitively perform. Image processing is applied in many fields that the main purpose is to emulate human vision, including learning and decision making according to the perceived data (GONZALEZ and WOODS, 2008). Image processing has two purposes according to its applications: (1) improve the appearance of images for the user and (2) extraction of characteristics and information of images

The recognition of characteristics is often the main purpose of image processing. There are innumerous methods for identifying characteristics. Those characteristics can be color, shape, texture, structures, luminosity or a mixture of these.

Fundamentals of digital image processing

Image processing is a process that involves several steps of analysis. The diagram depicted in Figure 1 illustrates the fundamental steps in digital image processing.

Figure 4 – The fundamental steps in digital image processing

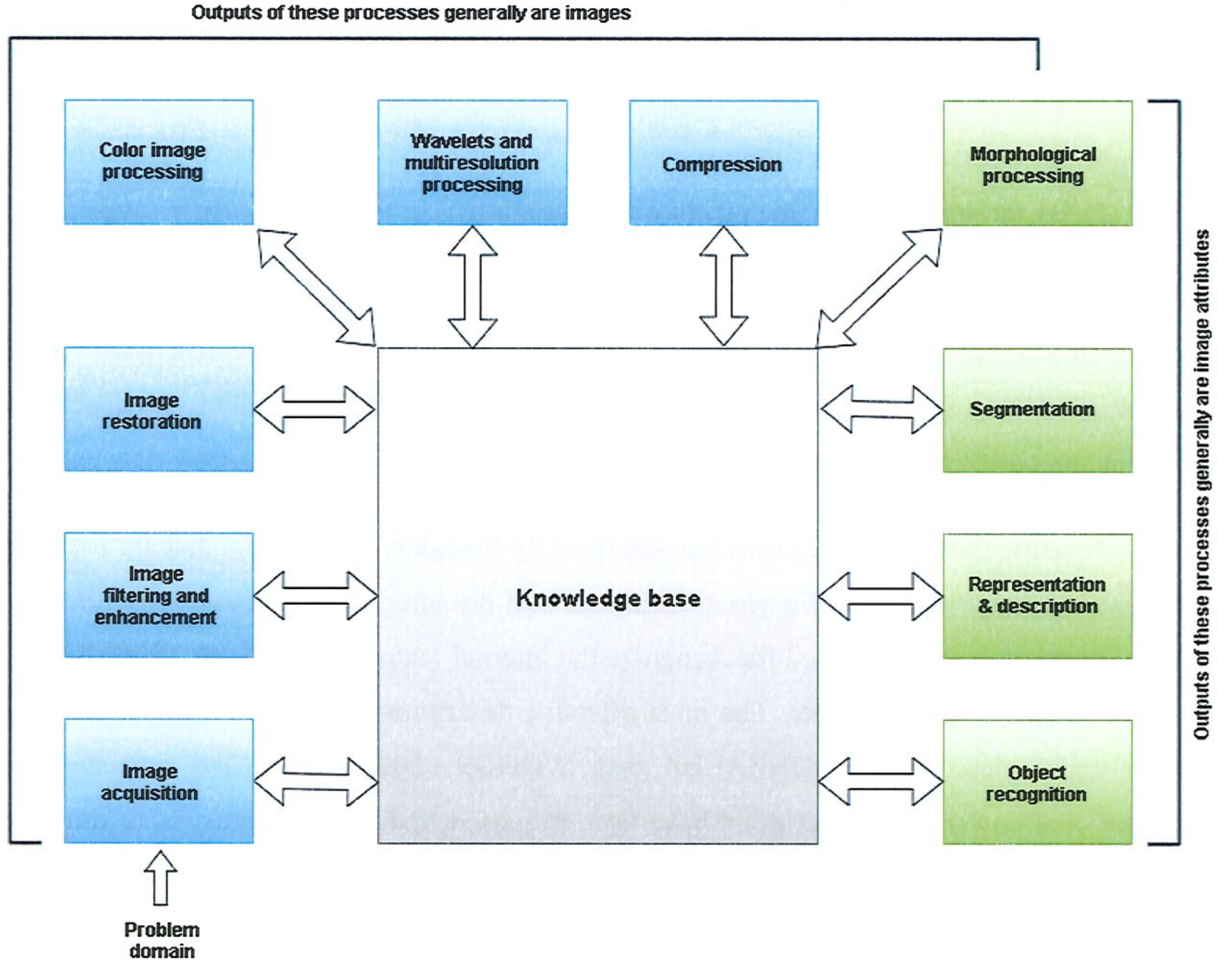
Outputs of these processes generally are images
Color image processing
Wavelets and multiresolution processing
Compression
Morphological processing
Image restoration
Segmentation
Knowledge base
Image filtering and enhancement
Representation & description
Image acquisition
Object recognition
Problem domain
Outputs of these processes generally are image attributes

Source – Adapted from Gonzalez and Woods (2008)

In the Figure 4, the diagram shows all operations that can be performed by means of image processing. The blue boxes represent those operations where the purpose of image processing is to improve the visual properties of the image, usually the outputs of these operations are images with higher quality that the original image. On the other hand, the green boxes represent the operations where the purpose of image processing is to extract information from the image, usually the outputs of these operations are vectors that describe the characteristics and patterns of the image.

Representation and description of objects at digital images

Many applications in image processing are programs capable of recognize certain features and patterns in images. Recognition of objects in digital images is part of many purposes, such as facial recognition, biometric identification, recognition of letters and numbers, etc. (GONZALEZ and WOODS, 2008).

In a nutshell, the objects in images can be described in two ways:

1) By external features (limits)
2) By internal features (the pixels within a region)

In a digital image, the objects are represented by a set of pixels. The characteristics of an object in a digital image can be described through a descriptor vector. The descriptor vector is constructed by a set of numeric data specific to a group of pixels, which is capable of describing an object in any condition.

Usually, the external features are described by boundary descriptors, that are used for recognize the shape features of a group of pixels, and the internal features are described by regional descriptors, that are used for recognize the internal features of a region of pixels such as color, texture, appearance, etc. The most effective descriptors describe objects combining two or more descriptors (GONZALEZ and WOODS, 2008). With the advances of computational power, new descriptors have been proposed, reducing the processing time for feature extraction. The identification process depends on the precision in the extraction of invariant features. According to Gonzalez and Woods (2008), an effective descriptor has the following characteristics:

1) Must be defined by a complete group of pixels
2) Be congruent
3) Must have invariant properties
4) Must have recognizable features regardless modifications in the images
5) Be compact
6) Having a set of exact features

Object recognition

Object recognition is performed for identifying patterns. A pattern is an arrangement of some descriptors. The pattern classes are a set of descriptors that have common properties. Computer-aided identification includes techniques for organizing the patterns in classes automatically.

A pattern is represented as a vector as follows:

$$\boldsymbol{\rho} = [\delta_1 \; \delta_2 \; \vdots \; \delta_n \;] \tag{1}$$

where $\boldsymbol{\rho}$ is the pattern, each component $\boldsymbol{\delta_n}$ represents the n-th descriptor and n is the total number of descriptors associated with the pattern. Figure 5 illustrates the process for the recognition of patterns in digital images.

Figure 5 – Recognition by patterns

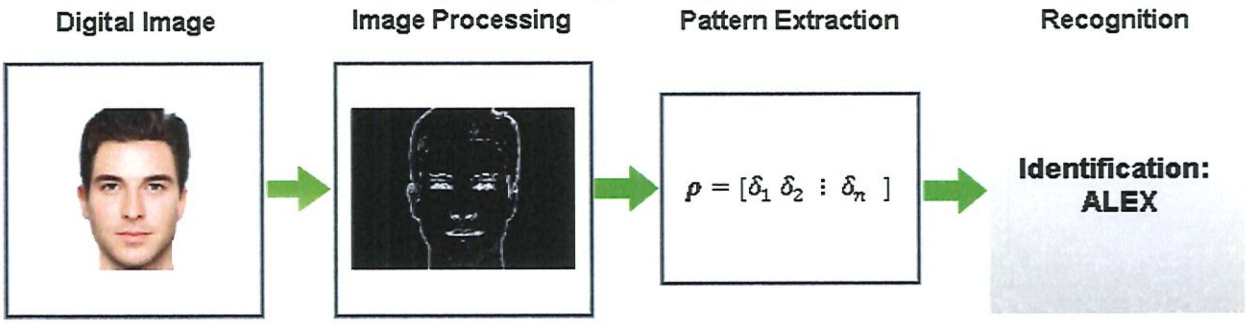

Source – Created by the author

The nature of the pattern depends on the approach used to describe the physical features. The following example described in Gonzalez and Woods (2008) is presented to illustrate this concept.

Three types of flowers are presented: Iris Setosa, Iris Virginica, and Iris Versicolor. The characteristics of the widths and the lengths of every flower were extracted using boundary descriptors by the computational vision method. The pattern used to recognize the flowers is constructed using two descriptors: the length and width of its petals, δ_1 and δ_2, respectively:

$$\boldsymbol{\rho} = [\delta_1 \; \delta_2 \;] \tag{2}$$

The descriptors δ_1 and δ_2 allow the identification of the Iris Setona from the other types of flowers, as shown in the Figure 6. However, the Iris Virginica and Iris Versicolor cannot be classified using only these two boundary descriptors. This identification would require a regional descriptor that identify the color, texture or appearance of the petals.

Figure 6 – Types of flowers described by two descriptors

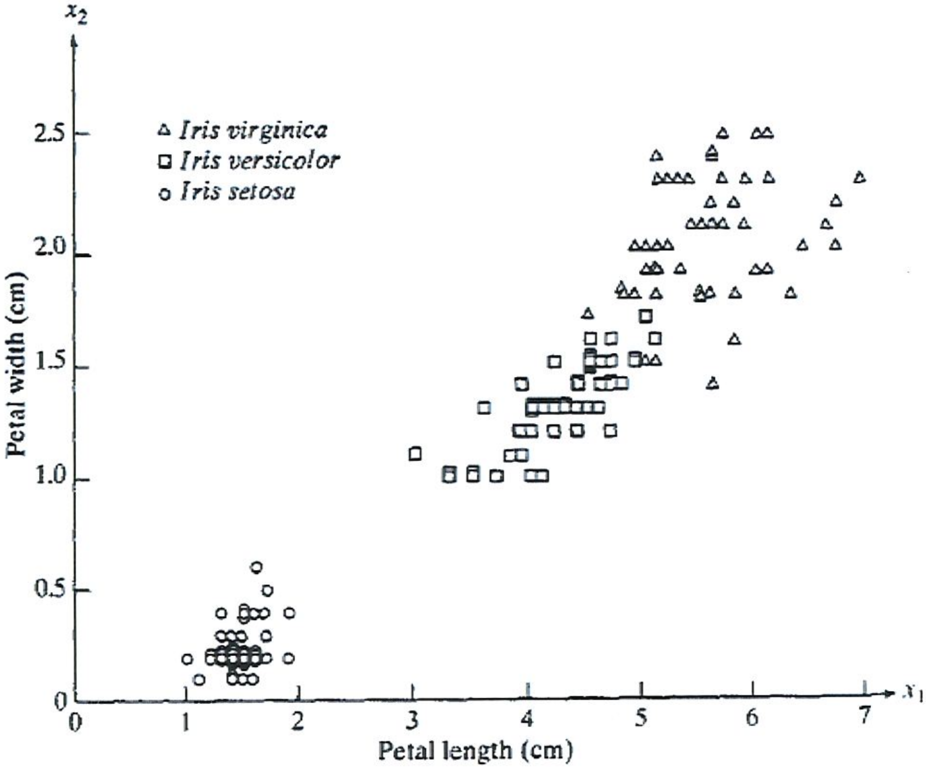

Source – Gonzalez and Woods (2008)

3.2 Recognition and location of internal corners of planar checkerboard pattern

The recognition and location of a checkerboard pattern is an important task for the calibration of the stereo camera method and the pinhole camera method. An effective proposal was developed by WANG *et al.* (2007) to recognize automatically the corners of a checkerboard. This approach is based on the local intensity and the grid line architecture of the corners. The process requires the assessment of the planar checkerboard pattern (see Figure 7) in different locations and positions.

Figure 7 – Planar checkerboard pattern

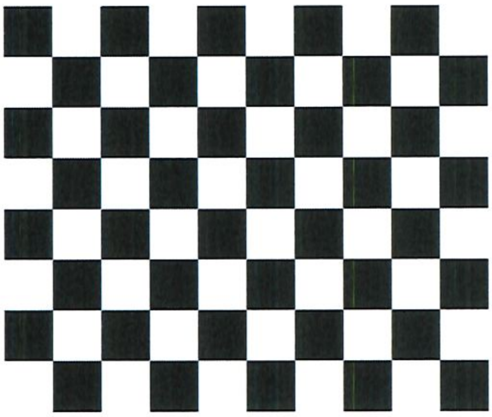

Source – Created by the author

One approach to process the checkerboard is to find the edges and fit lines. The corners are detected as the intersection of the edges of the white and black squares. The disadvantage of this method is that the edges are curved due to the radial distortion of the images. Bouguet (2004) developed an interesting approach to find the corners. The method had an automatic mechanism to count the number of squares in the checkerboard. Wang *et. al* (2007) proposed that the detection of the corners could be done by the identification of the intersections of black and white squares. Both methodologies are implemented in Matlab and are described in Sections 3.2.1 and 3.2.2, respectively.

The first step in the procedure is to load several images of the checkerboard pattern. The software automatically extract the internal corners from the images and match them all using the pattern of the corners. Knowing the physical dimensions of each square of the checkerboard, a correspondence between the 2-D points in the images and the dimensions of the checkerboard is established. With this correspondence, the application calculates the parameters of the stereo camera or the pinhole camera model by numerical procedures (HARTLEY and ZISSERMAN, 2003, cap. 8). Figure 8 shows the detection of the checkerboard in a digital image. The green dots are the detected corners of the checkerboard. The yellow dot is the origin point of the corners arrangement of the checkerboard.

Figure 8 – Checkerboard pattern detection by internal corners using the single camera calibration application (Matlab)

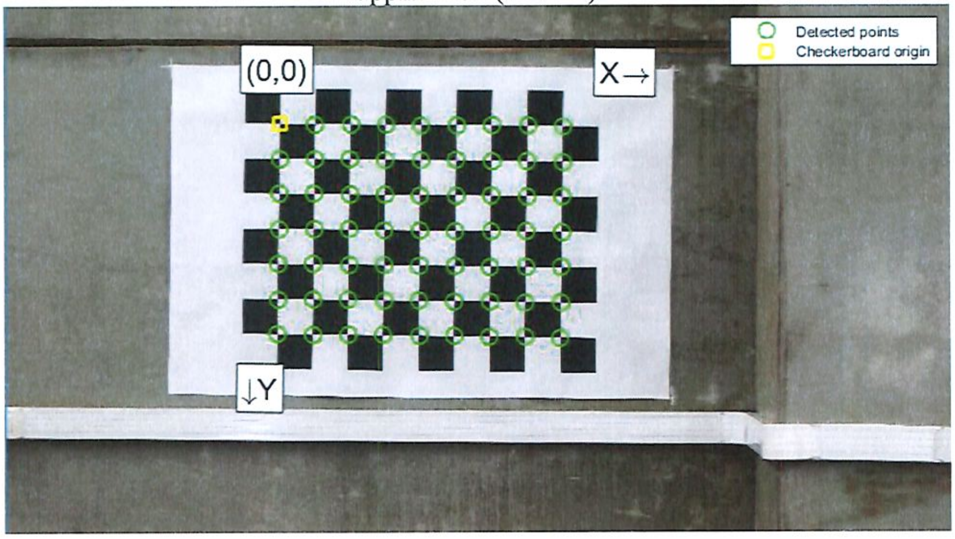

Source – Created by the author

3.2.1 Procedure to recognize a checkerboard pattern using Matlab

The procedure of the recognition of the internal corners has the following steps:

1) Detect all the corners in the planar checkerboard by exploiting the corner detector developed by Harris and Stephens (1988).
2) Recognize the corners at the intersections of black and white squares using the intensity of the planar checkerboard (WANG *et al.*, 2007, p. 5).
3) Recognize the corners at the intersections of two groups of grid lines based on the grid architecture (WANG *et al.*, 2007, p. 6).

3.2.2 Location of the internal corners of checkerboard pattern

The location of the internal corners of planar checkerboard is determined by the row and column of the corners in the array, and the origin point of the reference frame attached to the checkerboard. The process to localize the internal corners of the array has two steps:

1) Arrange the internal corners of the checkerboard
2) Determine the origin point of the reference checkerboard

Figure 9 illustrates the detection of the corners of the checkerboard pattern with the camera at an oblique angle.

Figure 9 – The arrangement of internal corners and the origin point

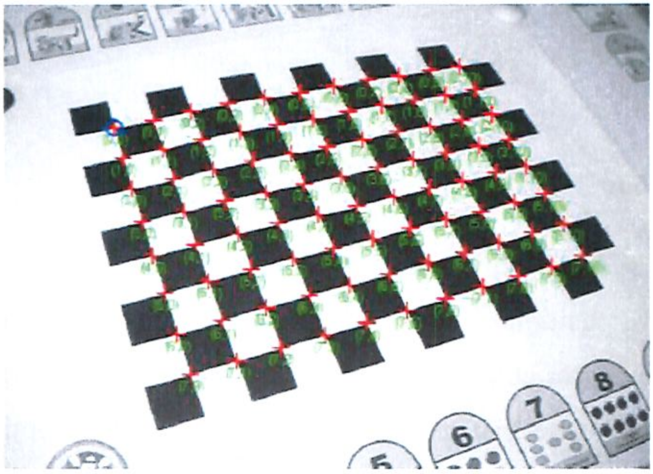

Source – Wang *et al.* (2007)

Wang *et al.* (2007) verified the pattern identification and calibration algorithms available at Matlab for a set of images of a checkerboard. The algorithms were applied to a set of 20 images with resolution of 640x480 pixels, using a checkerboard pattern of 14x13 squares that include 156 internal corners.

In Figure 10, the results and errors of the calibration are presented using the two different methods: an interactive method proposed by Wang *et al.* (2007) and image processing toolbox in Matlab.

Figure 10 – Results and errors of calibration

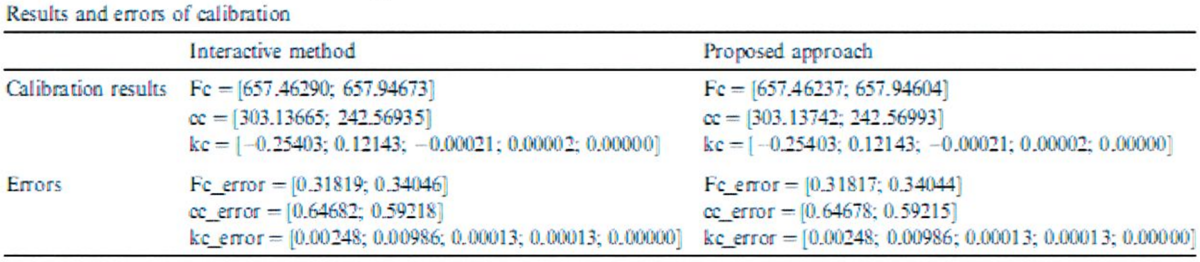

Results and errors of calibration

	Interactive method	Proposed approach
Calibration results	Fc = [657.46290; 657.94673] cc = [303.13665; 242.56935] kc = [−0.25403; 0.12143; −0.00021; 0.00002; 0.00000]	Fc = [657.46237; 657.94604] cc = [303.13742; 242.56993] kc = [−0.25403; 0.12143; −0.00021; 0.00002; 0.00000]
Errors	Fc_error = [0.31819; 0.34046] cc_error = [0.64682; 0.59218] kc_error = [0.00248; 0.00986; 0.00013; 0.00013; 0.00000]	Fc_error = [0.31817; 0.34044] cc_error = [0.64678; 0.59215] kc_error = [0.00248; 0.00986; 0.00013; 0.00013; 0.00000]

Source – Wang *et al.* (2007)

Figure 11 shows the time cost to process the 20 images by using these two different methods. The checkerboard identification using the Matlab toolbox took little computational cost compared to an interactive method.

Figure 11 – Computational time cost

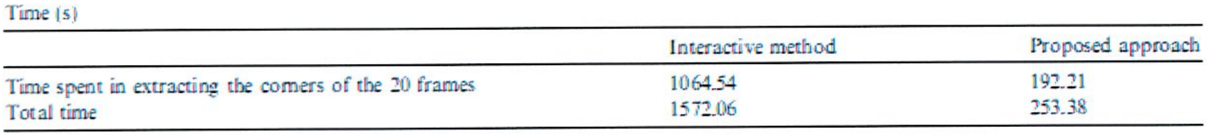

Time (s)	Interactive method	Proposed approach
Time spent in extracting the corners of the 20 frames	1064.54	192.21
Total time	1572.06	253.38

Source – Wang *et al.* (2007)

3.3 Stereo vision method

Stereo vision systems have many applications. The most used is the information extraction of the relative position of objects near of autonomous systems in space. Figure 12 shows the stages for the construction of a stereo system. Rectification is the initial process used to project the stereo images into a plane parallel to a line between the optical centers of images.

Figure 12 – Stages of stereo system construction

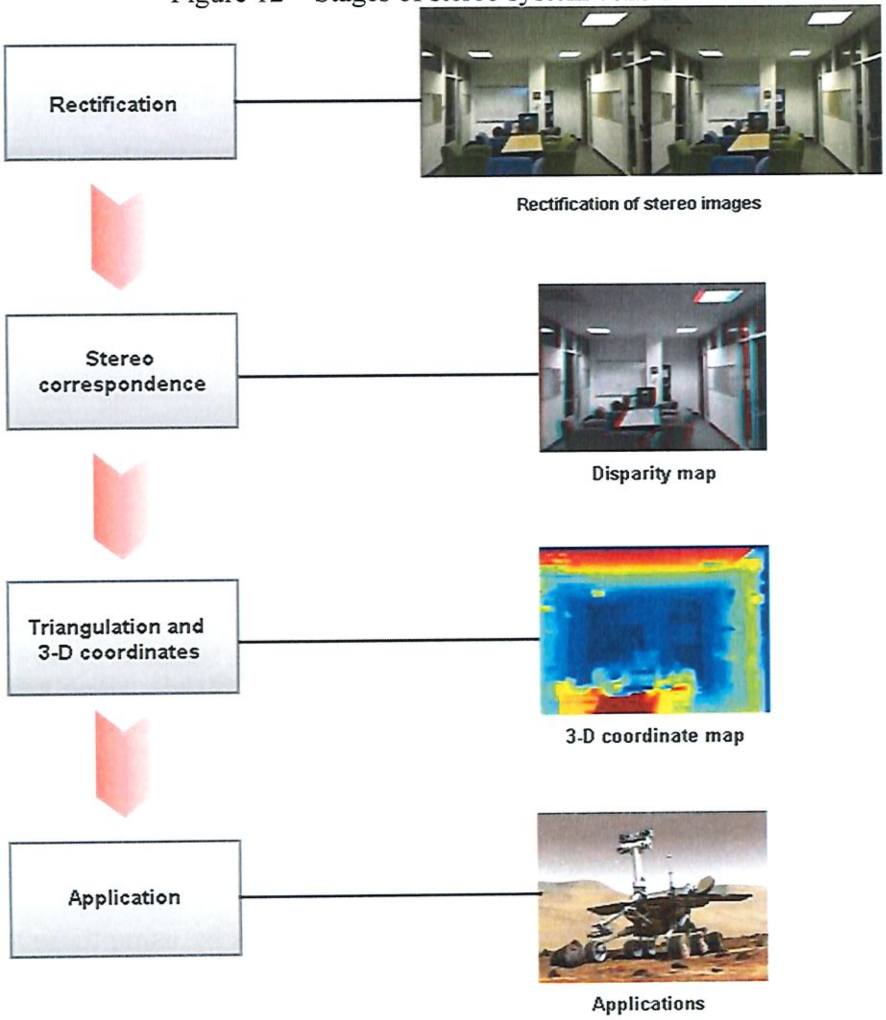
Rectification
Rectification of stereo images
Stereo correspondence
Disparity map
Triangulation and 3-D coordinates
3-D coordinate map
Application
Applications

Source – Created by the author

Stereo correspondence is the process of ascertaining which points in an image corresponding to the points in the other image. There are two main classes of algorithms using computational vision to find the correspondence between the stereo images.

- Correlation-based: establishes the correspondence by the intensity of the images in certain regions.
- Feature-based: establishes the correspondence by matching a sparse set of image features.

Triangulation and 3-D coordinates are the process of finding the 3D coordinates of the points in a stereo scene. To solve this problem, it is necessary to know the parameters of the stereo system. The transformation of a scene in 2-D plane to a 3-D plane is performed by the camera matrices found during the calibration process.

3.3.1 Stereo geometry

The stereo vision consists of two images, one image is considered as a reference image and the other one as an objective image. Therefore, each pixel of the reference image has its corresponding in the target image (stereo correspondence). The distance (measured in pixels) of a matching point between the reference image and the target image is known as disparity. When all the matching points are found, the disparity map has been completed (MATTOCCIA, 2011).

Epipolar geometry is defined as the geometry of stereo vision when two cameras observe a scene in different positions. There are a number of geometric relations between the 3-D points and their projections in 2-D images that lead to restrictions between the pixels of the stereo images. With two images, it can be set the 3-D coordinates of a point in a scene if the matching process is performed correctly. Figure 13 shows a scheme of the epipolar geometry between the images of a stereo system. The points Q and P are in the same red line of sight of the plane π_R at the reference image. The epipolar constraints establish that the points Q and P in the red line of sight corresponding to the points q and p in the green line of the plane π_T at the target image.

Figure 13 – Epipolar geometry

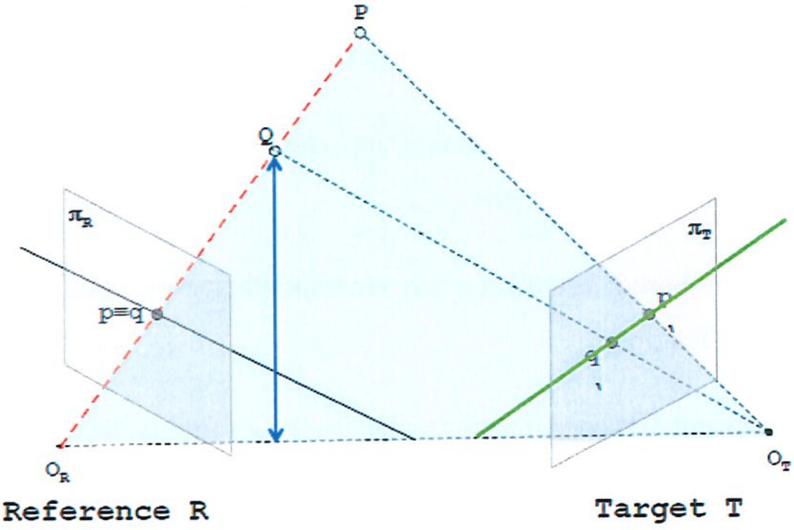
P
Q
π_R
p≡q
π_T
p'
q'
O_R
O_T
Reference R
Target T

Source – Mattoccia (2011)

When the search field for the matching points is known (by means of correspondence methods), the search field can be reduced from 2-D to 1-D. The images can be set in a convenient way (standard form, see Figure 14) and the matching points are constrained in the same image scanline. Figure 15 shows the correct alignment of stereo images when taken to standard form.

Figure 14 – Stereo system in standard form

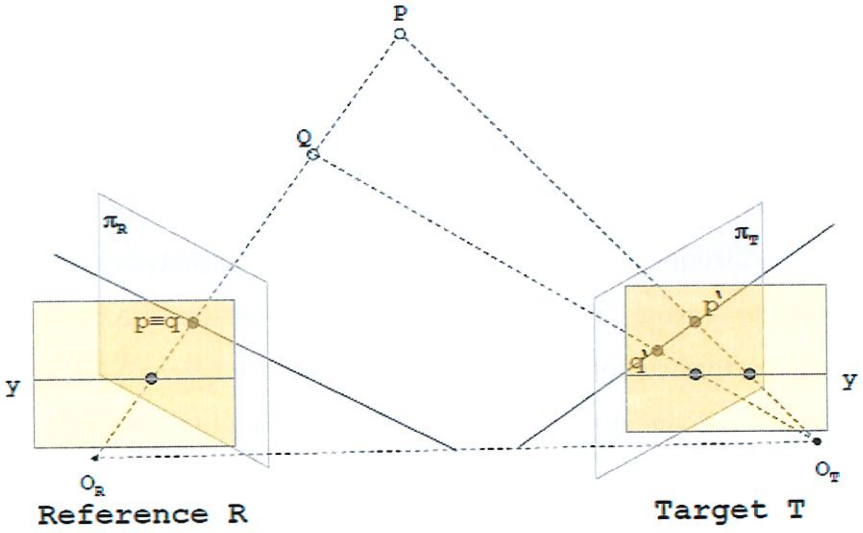
P
Q
π_R
p≡q
π_T
p'
q'
y
y
O_R
O_T
Reference R
Target T

Source – Mattoccia (2011)

Figure 15 – Stereo images in standard form with cameras correctly aligned

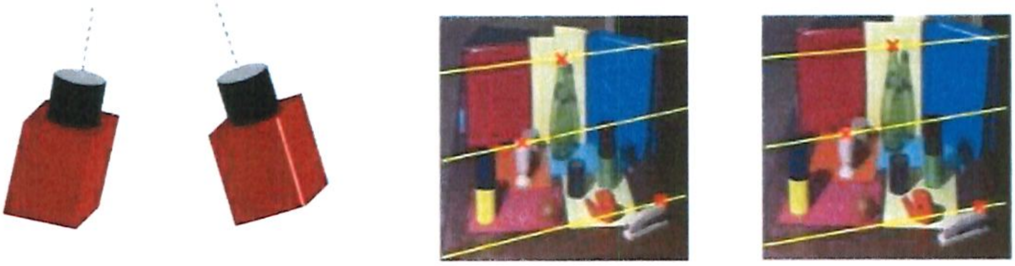

Original stereo pair

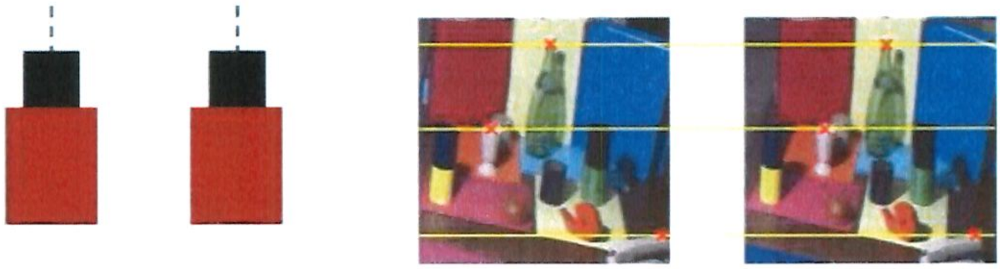

Stereo pair in standard form

Source – Mattoccia (2011)

3.3.2 Map of disparity and depth

Figure 16 shows the variables for calculating disparity of a point between the two views of a stereo image.

Figure 16 – Geometry of a stereo system

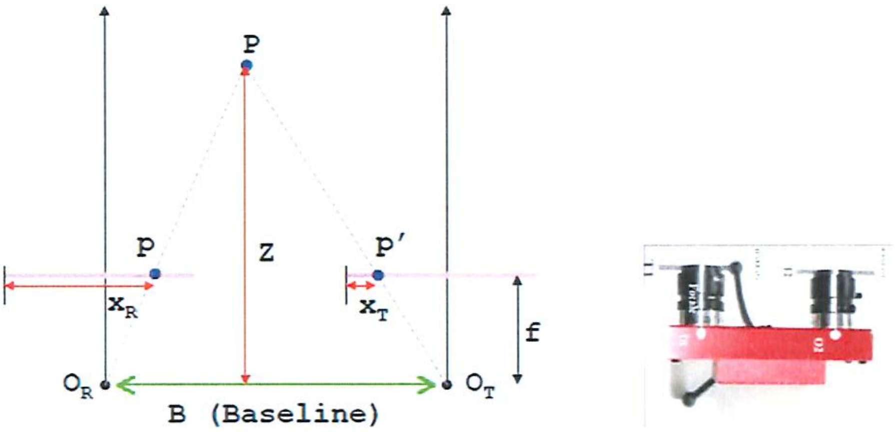

Source – Mattoccia (2011)

With the stereo system in standard form, the similar triangles PO_RO_T and Ppp' are considered and the depth z is calculated for all objects in the stereo image.

$$\frac{b}{z} = \frac{(b+X_T)-X_R}{z-f} \tag{3}$$

where:

b	Baseline, horizontal distance between camera lenses (mm)
z	Perpendicular distance of the camera to the point of perception (mm)
X_R	Side distance of object in perception in the reference image (mm)
X_T	Side distance of object in perception in the target image (mm)
f	Focal length of the stereo cameras (mm)

In this way, the depth z can be calculated:

$$Z = \frac{b*f}{X_R-X_T} \tag{4}$$

where $d = X_R - X_T$ is the disparity.

Figure 17 shows the relationship between both views of the stereo image and a same point in the scene.

Figure 17 – Disparity and depth in stereo vision

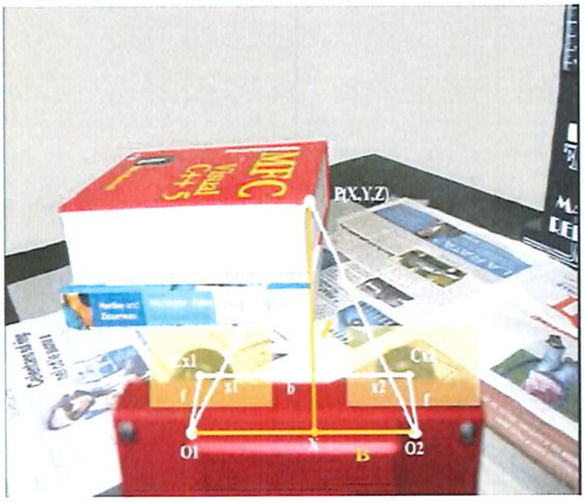

Source – Mattoccia (2011)

The disparity is the difference in pixels in the *x*-coordinate of the corresponding points between the stereo images. This difference is the key to obtain the disparity map typically encoded with grayscale images. Figure 18 shows the disparity map for a scene.

Figure 18 – Disparity map in stereo vision

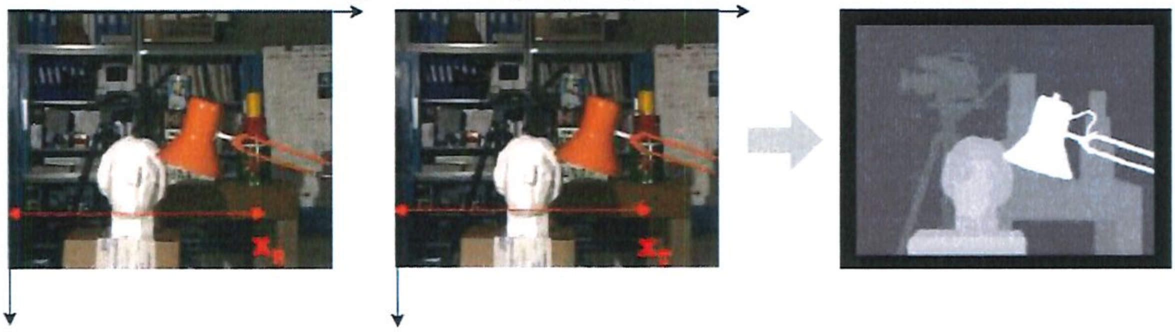

Reference image **Target image** **Disparity map**

Source – Mattoccia (2011)

The disparity is greater for points near the camera as shown in Fig. 19.

Figure 19 – Baseline between camera lenses

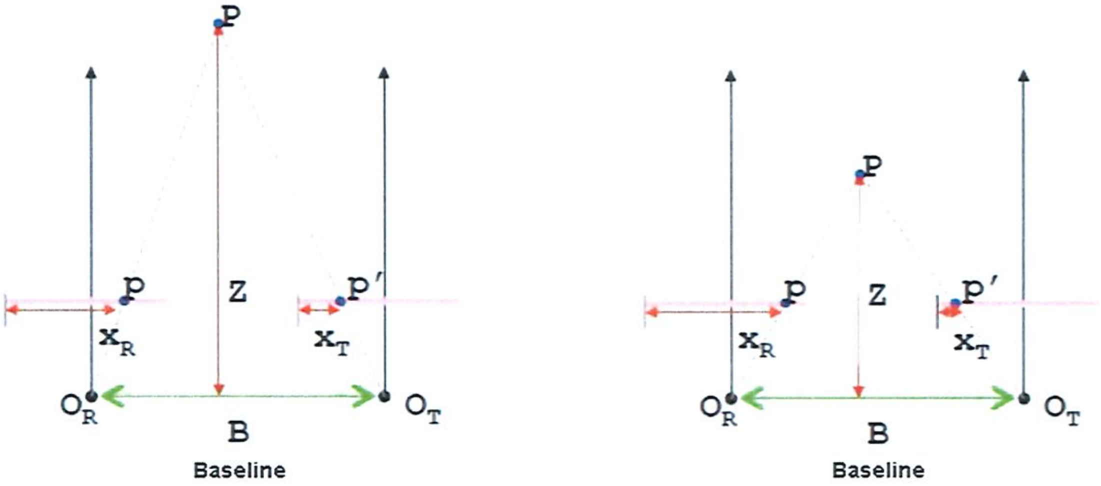

Source – Mattoccia (2011)

The stereo system has an operation field delimited by the parameters of the system. The parameters that intervene in the operation field are the baseline (*b*), focal length (*f*) and disparity values (d_{min}, d_{max}). Each matching point creates disparity value, each disparity value creates a plane that represents the perpendicular distance of the matching point respect to the stereo system. The operating distance of the stereo system is limited by a set of parallel planes, as shown in Fig. 20.

Figure 20 – Parallel planes with minimum and maximum distances of perception

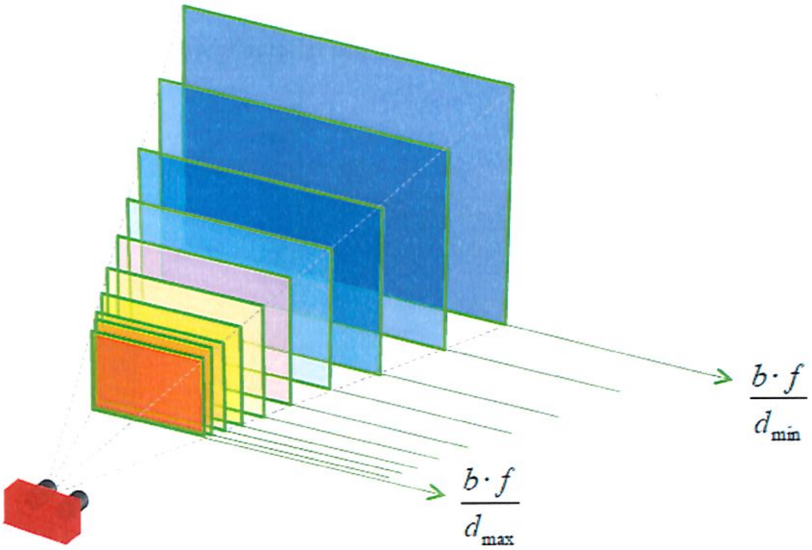

Source – Mattoccia (2011)

3.3.3 Calculating 3-D coordinates

The 3-D coordinates of all points in the disparity map are acquired through triangulation calculations. The calculations of these coordinates are given by:

$$Z' = \frac{b * f}{d} \tag{5}$$

$$X' = Z' * \frac{X_R}{f} \tag{6}$$

$$Y' = Z' * \frac{Y_R}{f} \tag{7}$$

where X', Y', and Z' are the coordinates of the points in the image respect to the stereo system. Figure 21 shows the transformation of all points of a 2-D scene into a 3-D field from the disparity map calculations.

Figure 21 – 2-D space to 3-D space conversion

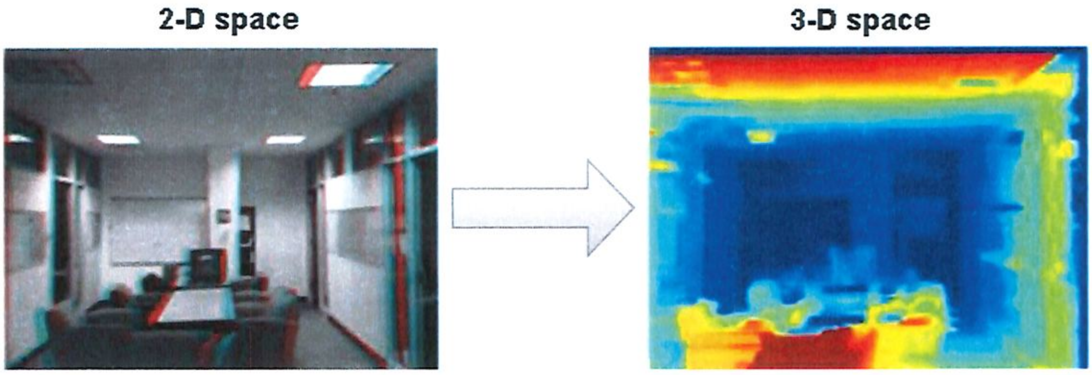

Source – Created by the author

3.4 Pinhole camera method

The parameters of the camera include intrinsic and extrinsic parameters, and distortion coefficients. The parameters are presented in a 4x3 matrix called the camera matrix (***P***). This matrix maps the 3-D scene in a two-dimensional plane. The extrinsic parameters of the camera are represented by the local coordinates of the camera in the 3-D scene. These parameters are rotation (***R***) and translation (***t***). The intrinsic parameters are represented by the focal center of the camera and the focal length of the lens, represented by the matrix ***K*** (see equation 8).

$$\boldsymbol{P} = [R\ t\,]K \tag{8}$$

$$w[x\ y\ 1\,] = [X\ Y\ Z\ 1\ \,]P \tag{9}$$

where:

w	Scale factor
$[x\ y\ 1\,]$	Image points
$[X\ Y\ Z\ 1\ \,]$	World points

The 3-D points of the scene are transformed to local coordinates of the visual system using the extrinsic parameters. Then, the camera location is mapped by using the image plane using the intrinsic parameters (as illustrated in Figure 22).

EESC • USP
Biblioteca
CAMPUS DE S. CARLOS

Figure 22 – Camera location mapping

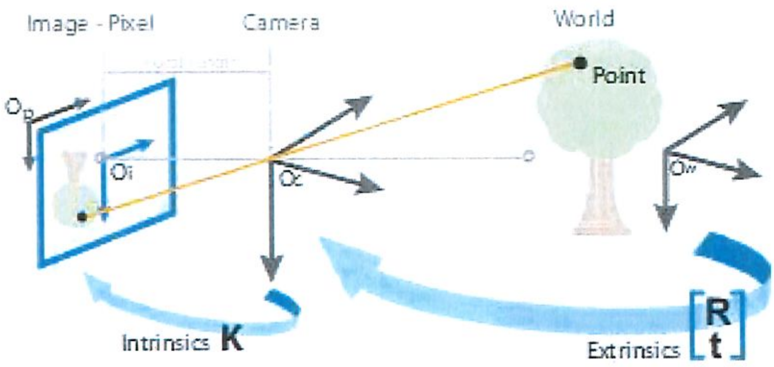
Image - Pixel
Camera
World
Point
Op
Oi
Oc
Ow
Intrinsics K
Extrinsics
R
t

Source – Mathworks (1994)

3.4.1 Calibration parameters

The calibration algorithm implemented in Matlab uses the extrinsic and intrinsic parameters and lens distortion to perform the calibration of a single camera (BOUGUET, 2004). The calibration algorithm also calculates the camera matrix. The extrinsic factors perform the transformation from the 3-D world coordinate system to the 3-D camera's coordinate system. Consequently, the intrinsic parameters represent a projective transformation from the 3-D camera's coordinates into the 2-D image coordinates. This process is illustrated in Figure 23.

Figure 23 – Camera location mapping process

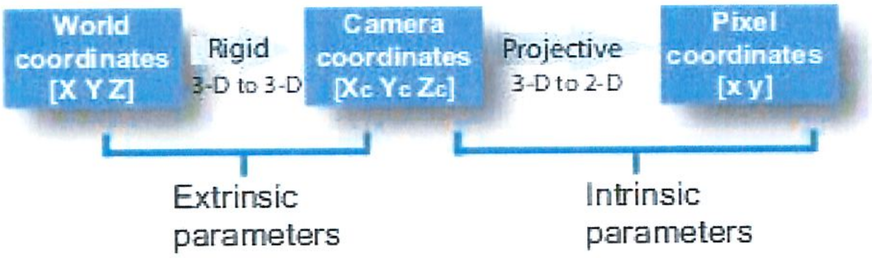
World coordinates [X Y Z]
Rigid
3-D to 3-D
Camera coordinates [Xc Yc Zc]
Projective
3-D to 2-D
Pixel coordinates [x y]
Extrinsic parameters
Intrinsic parameters

Source – Mathworks (1994)

3.4.2 Extrinsic parameters

The extrinsic parameters consist of a rotation (***R***) and a translation (***t***). The origin of the global 3-D coordinate system is the focal center (*x*, *y*) define by the checkerboard plane.

Knowing the checkerboard plane, and the parameters of rotation and translation of the visual system it is possible to know the location of the camera in the space.

Figure 24 – Extrinsic parameters of the camera

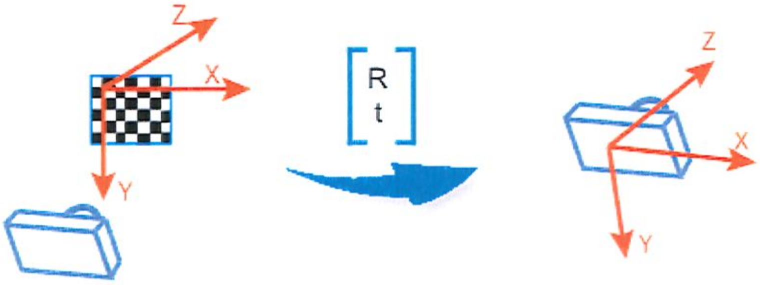

Source – Mathworks (1994)

3.4.3 Intrinsic parameters

The intrinsic parameters of the camera are the focal length, the optical center, and skew coefficient. The matrix of the intrinsic parameters (***K***) is defined as:

$$\boldsymbol{K} = \begin{bmatrix} f_x & 0 & 0 \\ S & f_y & 0 \\ c_x & c_y & 1 \end{bmatrix} \tag{10}$$

$$f_x = \frac{F}{p_x} \tag{11}$$

$$f_y = \frac{f}{p_y} \tag{12}$$

$$S = f_y \, tan \propto \tag{13}$$

where:

$[c_x \; c_y]$	Optical center (pixels)
$[f_x \; f_y]$	Focal length (pixels)
f	Focal length in measurement system (mm)
$[p_x \; p_y]$	Pixel size in measurement system (mm)
S	Skew coefficient

The skew coefficient is defined as illustrated in Figure 25, where P_x and P_y are the pixel lengths in the *x* and *y* coordinates, respectively, and α is the pixel distortion angle between the *x* and the *y* axis, and is often 0.

Figure 25 – Skew coefficient

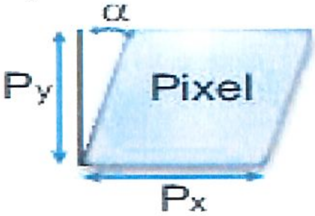

Source – Mathworks (1994)

3.4.4 Distortion in camera

The camera matrix (***P***) does not include optical lens distortion because a pinhole camera does not have lenses. To perform a simple camera approach, the calibration model developed by Bouguet (2004) includes the radial and tangential distortion of the lenses. The objective is to increase the accuracy of calibration and reduce errors due to lens distortion. Radial distortion occurs when light rays curl closer to the edges than they do from its optical center of the lens. Figure 26 shows this type of distortion.

Figure 26 – Types of radial distortions of lenses

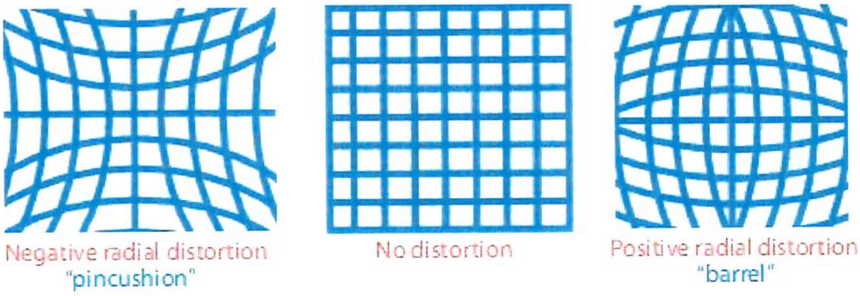

Source – Mathworks (1994)

The distorted points are defined as:

$$X_{Dis} = x(1 + k_1 * r^2 + k_2 * r^4 + k_3 * r^6) \tag{14}$$

$$Y_{Dis} = y(1 + k_1 * r^2 + k_2 * r^4 + k_3 * r^6) \tag{15}$$

where:

x, y	Location of the distorted pixels. x, y are normalized in coordinates of the images.
k_1, k_2, k_3	Radial distortion coefficients

In the equations 14 and 15, the variable r is defined as:

$$r = \sqrt[2]{x^2 + y^2} \tag{16}$$

Tangential distortion occurs when the lens and the plane of the image are not parallel. Figure 27 illustrates this type of distortion.

Figure 27 – Tangential distortion of lenses

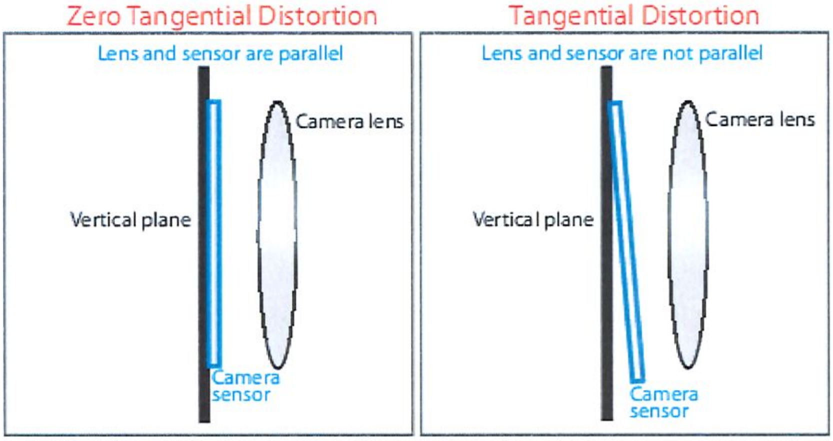
Zero Tangential Distortion
Lens and sensor are parallel
Camera lens
Vertical plane
Camera sensor
Tangential Distortion
Lens and sensor are not parallel
Camera lens
Vertical plane
Camera sensor

Source – Mathworks (1994)

The tangential distortion points are defined as:

$$X_{Dis} = x + [2 * q_1 * x * y + q_2 * (r^2 + 2 * x^2)] \tag{17}$$

$$Y_{Dis} = y + [q_1 * (r^2 + 2 * y^2) + 2 * q_2 * x * y] \tag{18}$$

where:

x, y	Location of undistorted pixels. x, y are normalized in coordinates of the images
q_1, q_2	Tangential distortion coefficients

In the equations 23 and 24, the variable ***r*** is defined as:

$$r = \sqrt[2]{x^2 + y^2} \tag{19}$$

3.5 Evaluation of visual systems

The best way to evaluate the accuracy of a visual system is to perform an efficiency test which is a standard procedure. The test consists in measuring physically the coordinates of the checkerboard pattern with respect to the visual system (stereo vision or pinhole camera method) and then perform a comparison with the coordinates calculated using computational vision. With the Matlab calibration application this test can be done.

The Matlab application follows the following procedure:

1) Several images taken with the visual systems (stereo vision/ pinhole camera model) are inserted to the application of the toolbox of Matlab.
2) Detection of the checkerboard pattern in all the images.
3) Calculation and calibration of the parameters of the visual systems.
4) Calculation of the positioning coordinates of the visual system with respect to the checkerboard pattern.

The test scheme is shown in Figure 28. In this figure, X, Y, and Z are the real coordinates measured physically of the visual system respect to the checkerboard pattern, and X', Y' and Z' are the coordinates calculated by the software.

Figure 28 – System coordinates applied in the efficiency evaluation

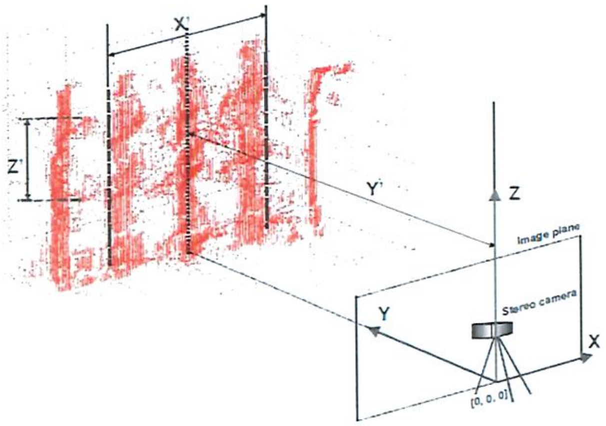

Source – ROVIRA-MÁS, WANG and ZHANG (2008)

There are many ways to compare the coordinates calculated by the software and the real coordinates. Rovira-Más, Wang and Zhang (2008) indicates that the most efficient way is to calculate error percentages at each coordinate as established in the following expressions:

$$\mathcal{E}_X = |\frac{X}{X\prime} - 1| * 100 \tag{20}$$

$$\mathcal{E}_Y = |\frac{Y}{Y\prime} - 1| * 100 \tag{21}$$

$$\mathcal{E}_Z = |\frac{Z}{Z\prime} - 1| * 100 \tag{22}$$

Equations 20, 21 and 22 show the percentage errors in each coordinate. The values are positive and provides precision information in one direction. The main objective is to determine the accuracy of visual systems at different ranges of distance up to the checkerboard pattern. The value η_{2D}, denoted as planar efficiency, calculates the accuracy of the visual systems at the coordinates X, and Z. The value η_{3D}, denoted as stereo efficiency, calculates the accuracy of the visual systems at the three coordinates (ROVIRA-MÁS, WANG and ZHANG, 2008). Both indices are provided in percentages and are calculated as follows:

$$\eta_{2D} = (1 - 0.01 * \mathcal{E}_X) * (1 - 0.01 * \mathcal{E}_Z) * 100 \tag{23}$$

$$\eta_{3D} = (1 - 0.01 * \mathcal{E}_X) * (1 - 0.01 * \mathcal{E}_Y) * (1 - 0.01 * \mathcal{E}_Z) * 100 \tag{24}$$

3.6 Evaluation of auto-guidance system

Once determining which visual system is the most accurate to accomplish our research objectives. The system was installed on the tractor, and using computational vision the position of the vehicle in the field was mapped taking as reference the checkerboard pattern fixed in the field. Multiple images were processed to validate the vehicle's position. For each frame, a vector with the 3-D coordinates relative to the tractor's location with respect to the reference checkerboard pattern was calculated. This vector was denoted as location vector $V_L (X_L, Y_L, Z_L)$. The vectors obtained from the digital frames were mathematically compared with their previous frames to calculate the motion of the vehicle at each coordinate. The Canon Rebel T5 camera is capable of acquiring 30 frames per second with a resolution of 1920x1088 pixels. As a result, the method offered 30 tractor's location data per second. Translations in the coordinates at the n-th frame were presented by the vector $T\ (T_x, T_y, T_z)$:

$$T_{xn} = X_{Ln} - X_{L(n-1)} \tag{25}$$

$$T_{yn} = Y_{Ln} - Y_{L(n-1)} \tag{26}$$

$$T_{zn} = Z_{Ln} - Z_{L(n-1)} \tag{27}$$

The absolute tractor's position was computed by taking the absolute coordinate as the location of the vehicle with respect to the checkerboard pattern. The local coordinate (0, 0, 0) of the visual system was located at the position of the checkerboard in the field. The coordinates of the position calculated using computational vision and requested to the GPS-RTK were transferred to UTM (Universal Transverse Mercator) coordinates in order to evaluate the auto-guidance system. The UTM uses a two-dimensional Cartesian coordinate system to furnish the positions on the surface of the earth. This coordinate system proves to be favorable to the methodology since the coordinates of the vehicle position are given by an own 3-D coordinate system when using the Image Processing Toolbox in Matlab.

The coordinates of the points A/B of the programmed line in the auto-guidance system were given in geographic coordinates. Then, the coordinates of the points A/B were transformed to UTM coordinates and the equation of the programmed line was calculated as a line on a Cartesian plane. According to the manufacturer, the geographic coordinates of points A/B provided by the auto-guidance system have a precision of 25 mm in UTM coordinates.

The data locations acquired by the visual system were translated to UTM coordinates using the following rotation and translation operators:

$$(\boldsymbol{X}_{UTM}, \boldsymbol{Y}_{UTM}) = \sum_{n=1}^{N} \left\| \begin{bmatrix} \cos\theta & -\sin\theta \\ \sin\theta & \cos\theta \end{bmatrix} \begin{bmatrix} X_n \\ Z_n \end{bmatrix} + \begin{bmatrix} T_{Xn} \\ T_{Zn} \end{bmatrix} \right\|^2 + \begin{bmatrix} ox \\ oy \end{bmatrix} \tag{28}$$

where:

$\boldsymbol{X}_{UTM}, \boldsymbol{Y}_{UTM}$	Tractor location in UTM coordinates, relative to longitude and latitude coordinates respectively
N	Total numbers of frames

θ	The rotation angle 2-D
$[T_{Xn}\ T_{Zn}]^T$	The translation in X and Z coordinates at each frame
$[ox\ oy]^T$	The location of the checkerboard in the field measured in UTM coordinates (was set as the location of point A of the programmed AB line obtained by the auto-guidance system)
$[X_n\ Z_n]^T$	The position coordinate of the n-th frame relative to the initial frame

Figure 29 illustrates the comparison between the GPS coordinate and the Camera coordinate for sake of comparison.

Figure 29 – Comparison and contrasting of location data of both systems

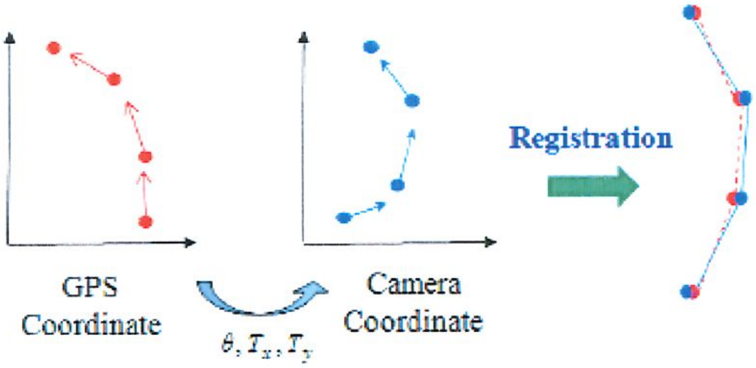

Source – Chon *et al.* (2011)

The auto-guidance system error is defined as the lateral distance of the vehicle's location with respect to the line programmed by the auto-guidance system. The auto-guidance system error was obtained calculating the distance between the tractor coordinates and the programmed line AB using the following equation:

$$\varepsilon_n = \frac{|A*X_{UTM(n)}+B*Y_{UTM(n)}+C|}{\sqrt{A^2+B^2}} \tag{29}$$

where:

ε_n	Auto-guidance error calculated in the n-th frame
A, B, C	Coefficients of the equation of the programmed line AB. $Ax + By + C = 0$
$(X_{UTM(n)}, Y_{UTM(n)})$	Location coordinates of the tractor at n-th frame

The average errors of the auto-guidance system were calculated at every operation speed to determine the precision of the auto-guidance system to the specific soil conditions of the field tests. In addition, the maximum amplitude of location of the tractor with respect to the programmed line AB was also calculated.

4 DESCRIPTION OF EXPERIMENTS

In this section, the experimental campaign is detailed. Firstly, the modeling of the visual systems are described. This description includes the modeling of both methods: the stereo vision and the pinhole camera. Secondly, the strategy for mapping the vehicle location in the field is explained. Thirdly, the vehicle's specifications are given for sake of completeness. Finally, the test and validation procedures are fully explained.

4.1 Modeling of the visual systems

4.1.1 Stereo vision method modeling

In this research, the stereo camera (also called stereo system) is built using two Canon Rebel T5 cameras with 50 mm focal lenses. The cameras are horizontally aligned to create a stereo image based by two views of a scene captured by the cameras. The parameters of the stereo system are described in Table 1.

Table 1 – Stereo system specifications

Cameras	Canon Rebel T5
Maximum baseline	955 mm
Minimal baseline	130 mm
Focal length	50 mm
Camera sensor	CMOS APS-C, 22.3 mm x 14.9 mm
Image resolution	5184 x 3456 pixels
Horizontal view angle	26°
Vertical view angle	17°
Image processing rate	30 frames/s

Source – Created by the author

The stereo camera calibration algorithm available in Matlab is used to calculate the parameters of the stereo system. In addition, the algorithm calculates the 3-D position of the stereo camera relative to the position of a checkerboard pattern. A large set of stereo images was used to calibrate the stereo system parameters and to calculate its position with respect to the checkerboard in any stereo pair. Figure 30 shows the stereo images taken at different distances from the checkerboard to perform the calibration of the stereo system in this research.

Figure 30 – Examples of stereo pairs loaded into the stereo camera calibration application (Matlab).

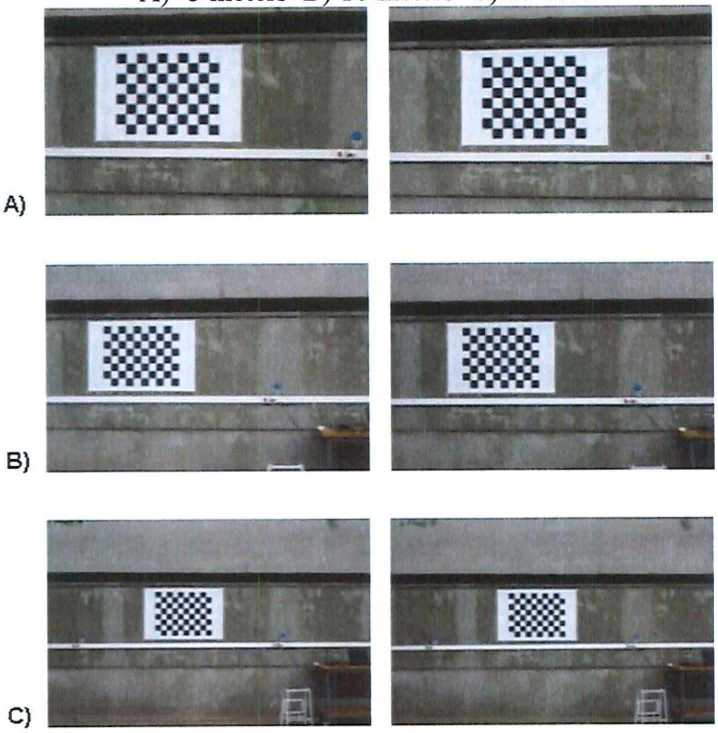

A) 5 meters B) 10 meters C) 15 meters

Source – Created by the author

In this research, a maximum allowed error of 50 mm of the stereo system was defined. The error of the location in the stereo camera method is defined as:

$$\varepsilon_{SV} = (\frac{Z^2}{fb}) d_{min} \tag{30}$$

where:

ε_{SV}	average location error (mm)
Z	perpendicular distance to the perception point (checkerboard pattern, mm)
f	focal length (pixels)
b	Baseline (mm)
d_{min}	minimum disparity value (pixels, usually $d_{min} = 1$)

Using the stereo camera calibration application of Matlab, the focal length of the Canon Rebel T5 camera with the 50 mm focal lens was 13235.88 pixels. The stereo system error is directly related to the perpendicular distance to the checkerboard pattern. Figures 31, 32, 33, and 34 depicts the average error vs. baseline at different distances. This determine which baseline is appropriate to calculate the location of the vehicle respect to the checkerboard pattern with a maximum error of 50 mm.

Figure 31 – Accuracy error vs baseline at 10 meters

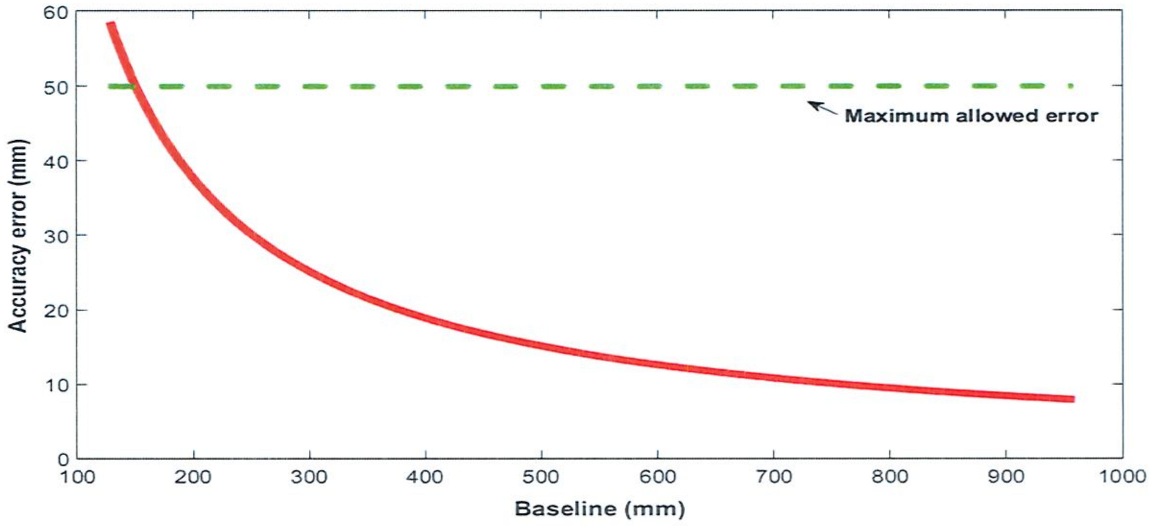

Source – created by the author

At 10 meters, for all the values of baseline allowed by the stereo system (between 130 and 955 mm) the system error remains under 50 mm. However, 10 meters is a short distance for testing the auto-guidance system.

Figure 32 – Accuracy error vs baseline at 15 meters

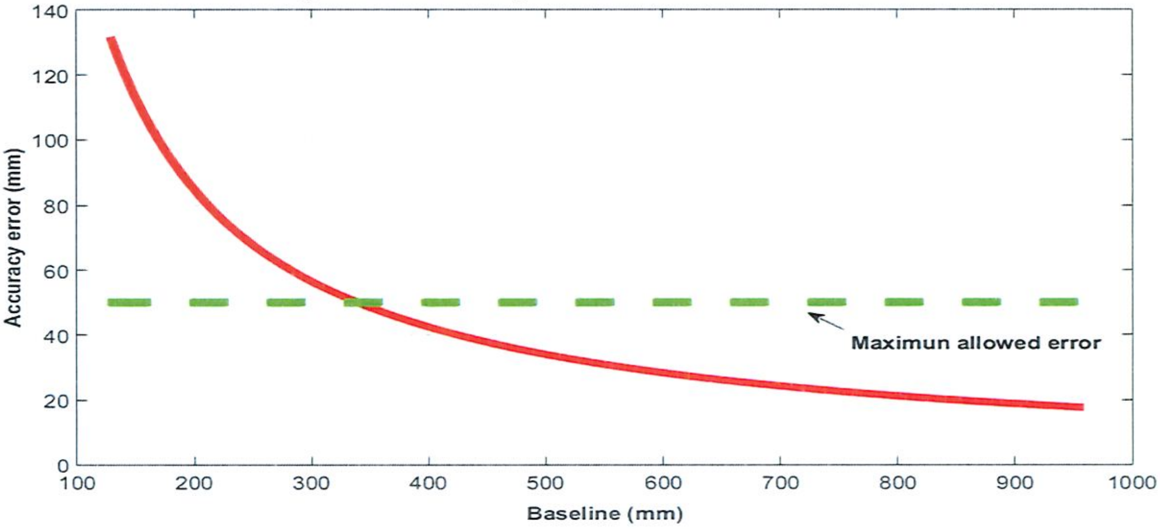

Source – Created by the author

At 15 meters, the stereo system error remains below 50 mm for baseline values between 350 and 955 mm. However, 15 meters remains being a short distance for testing the auto-guidance system.

Figure 33 – Accuracy error vs baseline at 20 meters

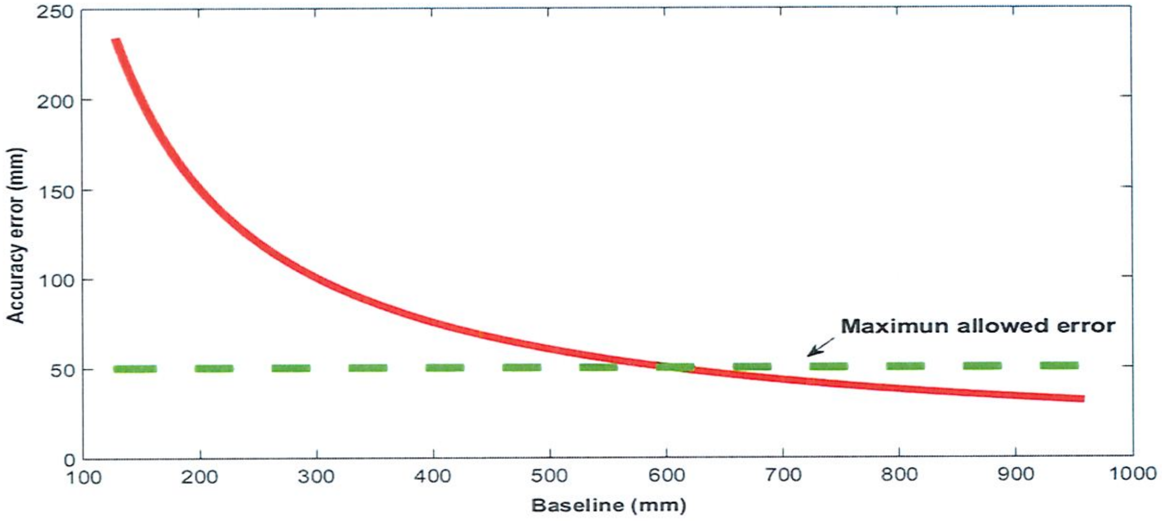

Source – Created by the author

At 20 meters, the stereo system error remains below 50 mm for baseline values between 620 and 955 mm.

Figure 34 – Accuracy error vs baseline at 25 meters

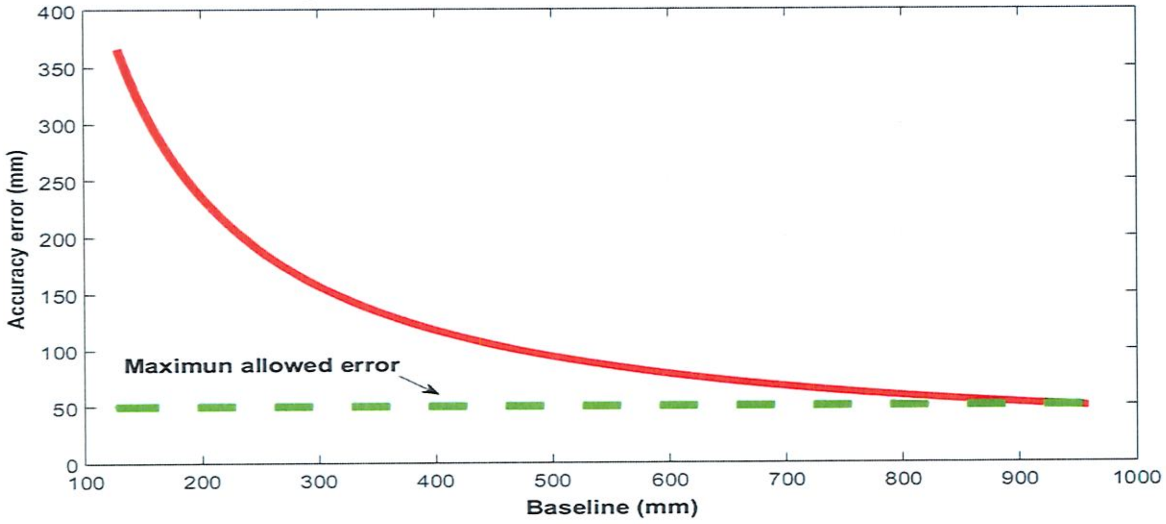

Source – Created by the author

At 25 meters, the stereo system error exceeds 50 mm for all the values of baseline allowed by the specifications of the system. However, a baseline of 950 mm allows the stereo system to have a 50 mm error (as shown in Figure 27).

Based on the theoretical calculations, the conclusion is that the stereo systems have a field of operation with high precision until 25 meters, after that, the system error exceeds the maximum permit in this research (50 mm). It is a fact that the stereo system error grows as the distance of perception increases. As a consequence, in order to increase the field of perception, a baseline of 950 mm was used with lenses of 50 mm. These choices resulted in a field of perception of 25 meters with a theoretical maximum error of 50 mm.

4.1.2 Pinhole camera method modeling

In this research, the single camera calibration available in Matlab was used to calibrate the parameters of the camera Canon Rebel T5 with 18mm focal lens. This calibration technique was proposed by Bouguet (2004) and includes the camera pinhole model and lens distortion. In addition, this application calculates the camera's position with respect to the checkerboard pattern. Figure 35 illustrates the pinhole camera model.

Figure 35 – Pinhole camera model

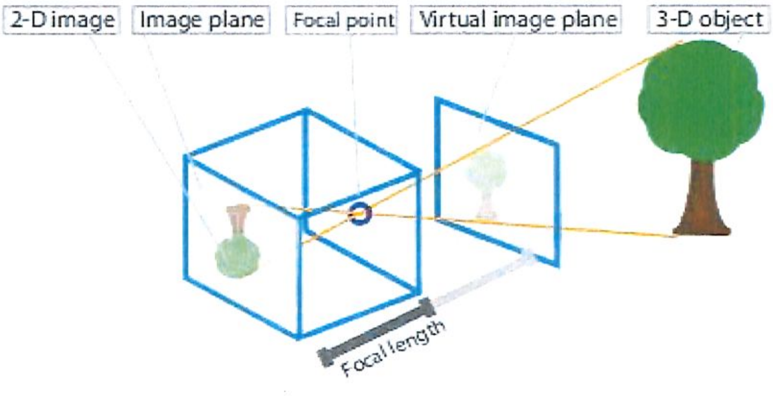

Source – Mathworks (1994)

The details of the camera pinhole method are in Table 2.

Table 2 – Camera pinhole method specifications

Camera	Canon Rebel T5
Focal length	18 mm
Camera sensor	CMOS APS-C, 22.3 mm x 14.9 mm
Image resolution	1920 x 1088 pixels
Horizontal view angle	64°
Vertical view angle	45°
Image processing rate	30 frames/s

Source – Created by the author

In the procedure, a set of images of the checkerboard in different positions and distances were uploaded to the software (as depicted in Figure 37). These images were used in the pattern detection algorithm, and then, to calculate the parameters of the camera. Once the parameters were assessed, it was possible calculate the position of the camera with respect to the checkerboard in any image.

Several images in the different positions of an arrangement of 40 x 40 centimeters (shown in Figure 36) were taken at distances of 5, 10, 15, 20, 25, 30, 35, and 40 meters respect to the checkerboard (shown in Figure 37), the objective was to assess the accuracy of the method at different distances. The corners are located at 100 mm from each other in the arrangement.

Figure 36 – Arrangement positioning for accuracy test

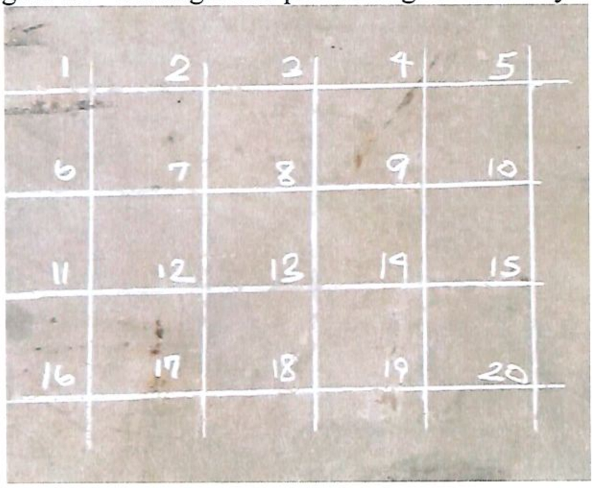

Source – Created by the author

Figure 37 – Set of images for the accuracy test (Camera pinhole method).
A) 5 meters B) 10 meters C) 15 meters D) 20 meters E) 25 meters F) 30 meters

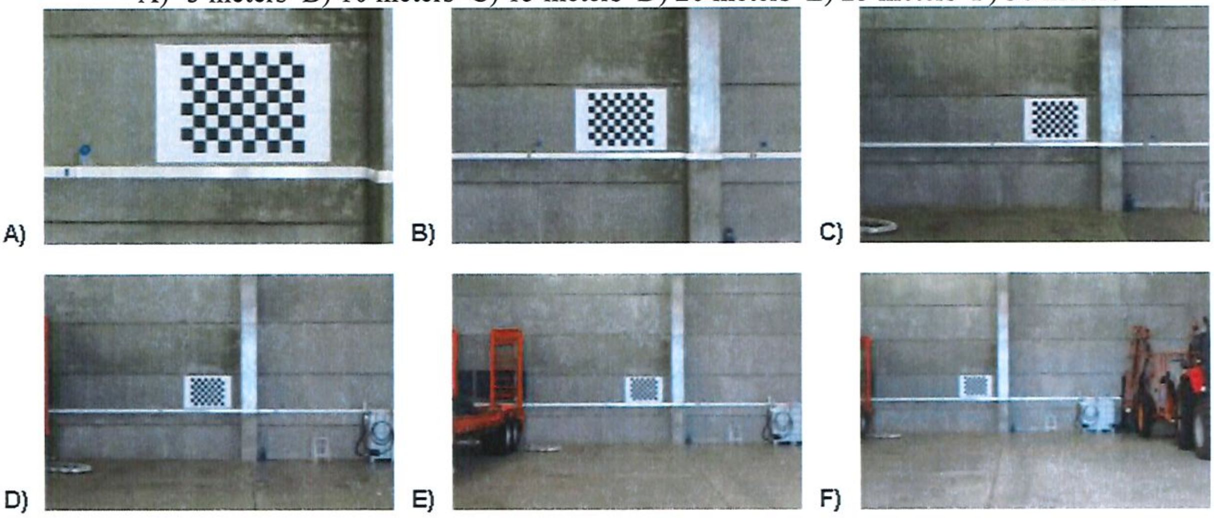

Source – Created by the author

An image of the checkerboard pattern was taken at each corner at different distances. This set of images was used to perform the calibration in Matlab and calculate the parameters of the camera. Then, the location of each image was calculated using the pinhole camera method and evaluate the accuracy of the method using the equations 23 and 24.

4.2 Mapping of the vehicle location in the field

The evaluation of auto-guidance systems requires a method for measuring the system's accuracy. Moreover, this method should be easy to use and reliable in any terrain situations. The relative position of the tractor with respect to the checkerboard installed in the field along a test track can be measured installing a visual system in the vehicle. This measurement was performed during the motion of the agricultural vehicle in auto-guidance mode. During this motion, several images of the checkerboard were acquired using a visual system installed on the back of the vehicle, as illustrated in Figs. 38 and 39. After performing the field tests, the image frames were loaded in Matlab and the data was treated using the Image Processing Toolbox. These images were used for calibrating the parameters of the visual system and assessing the location of the vehicle with respect to the checkerboard pattern. The camera video provides a high acquisition of images per second, reaching 30 frames per second with a resolution of 1920x1088 pixels.

Figure 38 – Single camera mounted on the test tractor

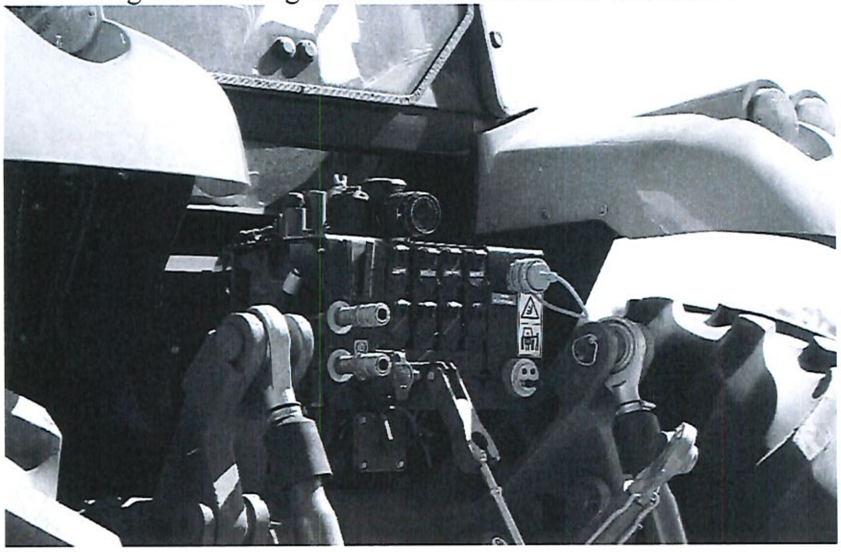

Source – created by the author

Figure 39 – Single camera mounted on the rear of the tractor

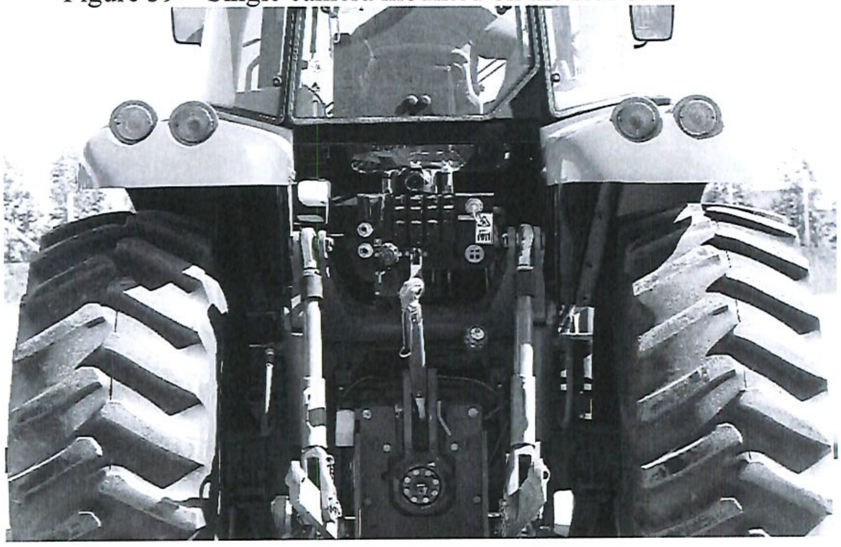

Source – Created by the author

4.3 Specifications of the tractor and auto-guidance system tested

Details of the vehicle and the auto-guidance system under study are given in Table 3.

Table 3 – Auto-guidance system specifications

Weight	8250 kg
Tractor power	159 hp
Nominal motor rotation	2200 rpm
Direction system	Hydrostatics
Dimensions (Length, Ext. Width, Height)	5365 mm, 2574 mm, 3210 mm
GPS Receiver	AGI-3
Satellite navigation system	GLONASS
GPS correction source	RTK
Inertial correction source	IMU system
RTK protocol	CMR
Antenna type	External
GPS output maximum rate	5 Hz
Geographic coordinate system	WGS84
Precision	25 mm

Source – Created by the author

4.4 The test procedure

The test procedure was carried out using a typical field operation. Firstly, the operator of the vehicle programmed an operation path (defined as a straight line AB). This path was programmed setting the points A/B using the auto-guidance system. Subsequently, the auto-guidance system replied this path repeatedly using the autonomous control system. The test path consisted of a 25-meter long straight line. During the tests, the maximum distance between the GPS RTK receiver in the tractor and the RTK base in the field was 100 meters. The error of the auto-guidance system was defined as the lateral difference between the programmed path and the real path performed by the vehicle in the auto-guidance mode. Figure 40 shows the test scheme used in this research.

Figure 40 – Desired programmed path and error of auto-guidance system

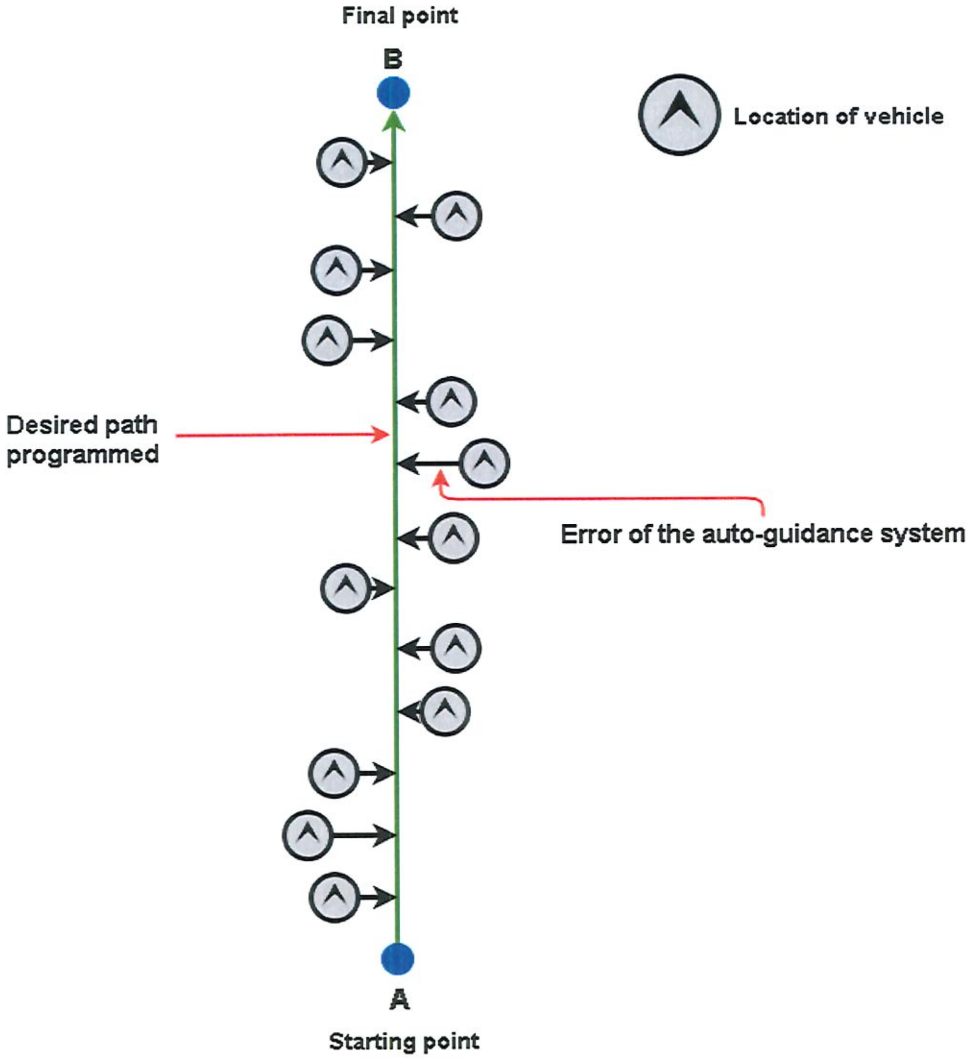
Final point
B
Location of vehicle
Desired path programmed
Error of the auto-guidance system
A
Starting point

Source – Created by the author

An appropriate test location should be a realistic terrain regarding the field conditions. In the test, the track was initially worked in order to perform a surface decompression, with the purpose that the wheels of the vehicle had a better adhesion. The terrain test track was located in the National Reference Laboratory for Precision Agriculture (LANAPRE, Embrapa Instrumentation) and is depicted in Fig. 41.

Figure 41 – The checkerboard pattern on the field at LANAPRE – Embrapa Instrumentation São Carlos

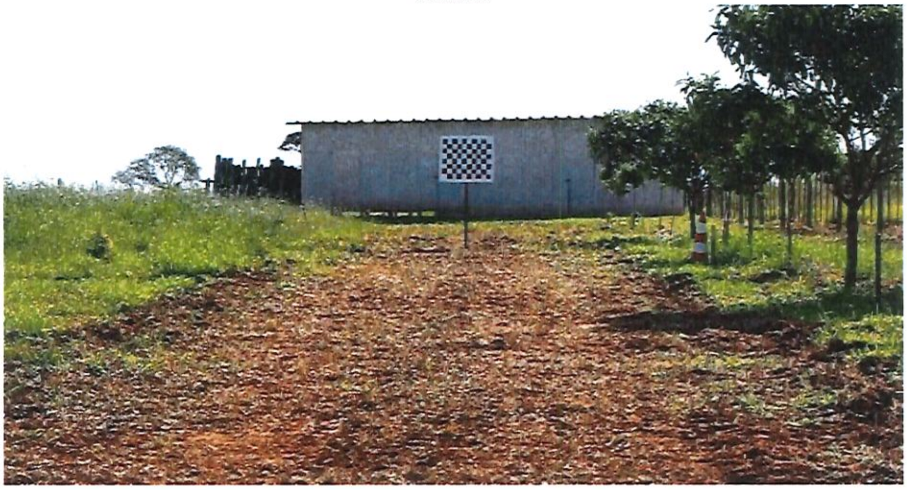

Source – Created by the author

For the test, the visual system was rigidly mounted at the rear of the vehicle chassis with the optical lens pointing towards the planar checkerboard pattern at the back of the vehicle. The accuracy of the auto-guidance system at real conditions were assessed at several usual speeds of operations. The vehicle was driven by the auto-guidance system in the track three times at each speed, although more tests could be performed, three tests were sufficient to determine an accurate estimate of the auto-guidance system evaluation. Table 4 describes the test conditions.

Table 4 – Field test specifications

Speed		Tractor gear	RPM	Number of Tests
m/s	km/h			
1,1	4	9	1500	3
1,25	4,5	9	1650	3
1,39	5	10	1550	3
1,53	5,5	10	1650	3

Source – Created by the author

All the frames were processed and the relative location of the tractor with respect to the reference checkerboard were measured. For each frame, the displacement of the vehicle was mapped and the error of the auto-guidance system was calculated using the mathematical calculations presented in the section 3.6.

4.5 Validation of the proposed methodology

This validation test aims to measure the accuracy of the auto-guidance system in a controlled environment where the surface conditions minimally affect the accuracy of the system. The second objective of this test is to validate the methodology proposed in this research by making a comparison with a standard methodology proposed by Easterly *et al.* (2010).

Easterly *et al.* (2010) proposed the use of a camera vertically located at the rear of the vehicle to capture the position of a straight line placed in the center of the drawbar hitch pinpoint when the tractor was moving in auto-guidance mode. With this method, it was possible to measure the deviation of the tractor's actual travel path from its desired path. The same strategy was performed in LANAPRE using a video. A rope was carefully stretched on a paved surface at a distance of 50 meters. The position of the camera and the rope are shown in Fig. 42.

Figure 42 – Camera vertically located at the rear of the tractor (validation test)

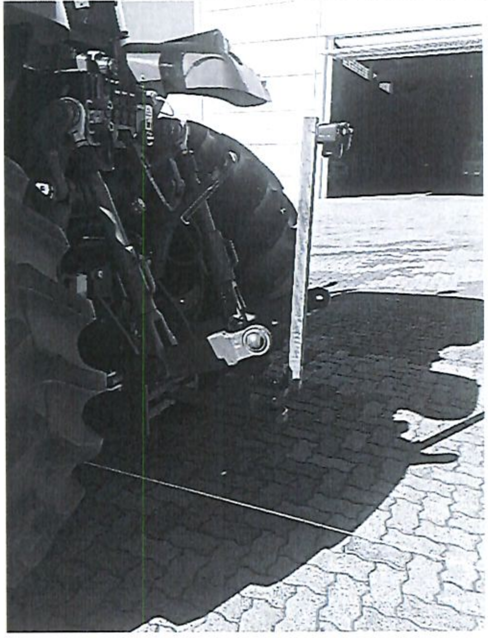

Source – Created by the author

Each frame of the video was processed using a segmentation method to identify the rope in each image. Then, the rope position was identified calculating the center of mass of the binary image, as depicted in Fig. 43.

Figure 43 – Detection of rope on the paved surface. A) Original image B) Processed image

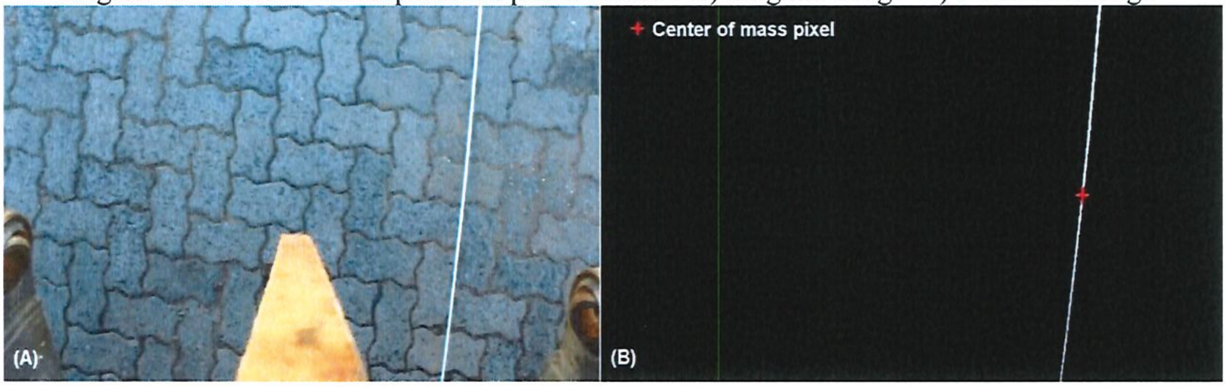

Source – Created by the author

The video acquires 30 frames per second. Since the lateral locations of the vehicle are given in millimeters, a calibration was required in order to assess the equivalence of a pixel to millimeters. To do this, an image of a checkerboard on the paved surface with the camera vertically positioned was taken (as depicted in Fig. 44). The distance between each corner of the checkerboard pattern was 29 mm and the number of pixels between each vertex was 56. In this way, each pixel was equivalent to 0.52 millimeters approximately. The size of the frames taken by the camera was 1920x1088 pixels.

Figure 44 – Checkerboard pattern using to calibrate the vertical located camera

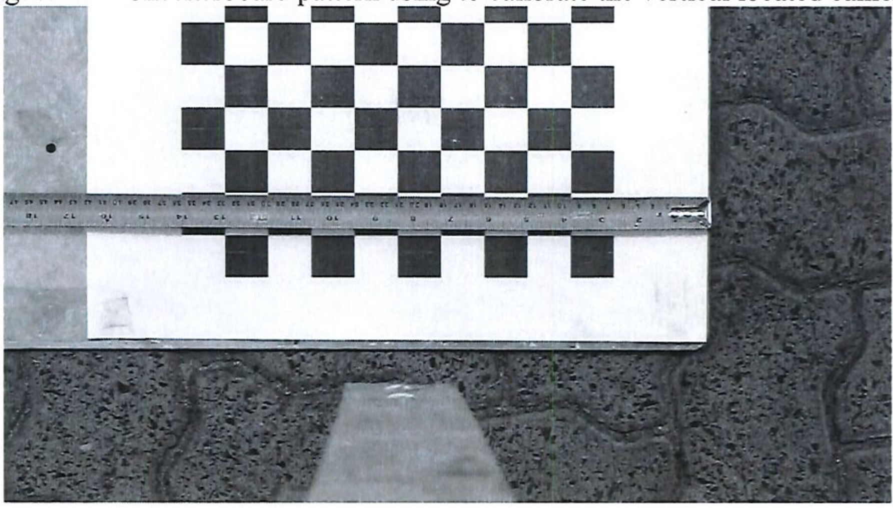

Source – Created by the author

A line was precisely programmed with the auto-guidance system setting the points A/B at two points along the rope. Subsequently, tests were performed with the auto-guidance system at speeds of 4.0 km/h, 4.5 km/h, 5.0 km/h, and 5.5 km/h comparing the methodology developed in this work with this validation methodology. During the tests, the maximum distance between the GPS RTK receiver in the tractor and the RTK base in the field was 100 meters.

5 RESULTS AND DISCUSSION

In this section, the results are presented and discussed. Firstly, a comparison between the stereo vision and the pinhole camera methods is performed. From this comparison, one can conclude that the stereo vision may not be fully adequate for this application. Therefore, the mapping of the vehicle's location in field operation is done by using the pinhole camera method. Finally, the validation of this proposed strategy is done by comparing it with a well-established methodology.

5.1 Accuracy evaluation Stereo Vision Method - Camera Pinhole Method

5.1.1 Stereo vision method

Several images were taken to detect the checkerboard and calculate its 3-D coordinates respect to the stereo system at distances between 5 and 10 meters. Figure 45 shows the results of this test, the planes of different colors represent the location of the stereo system respect to the checkerboard pattern.

Figure 45 – Accuracy tests with stereo vision method until 10 meters

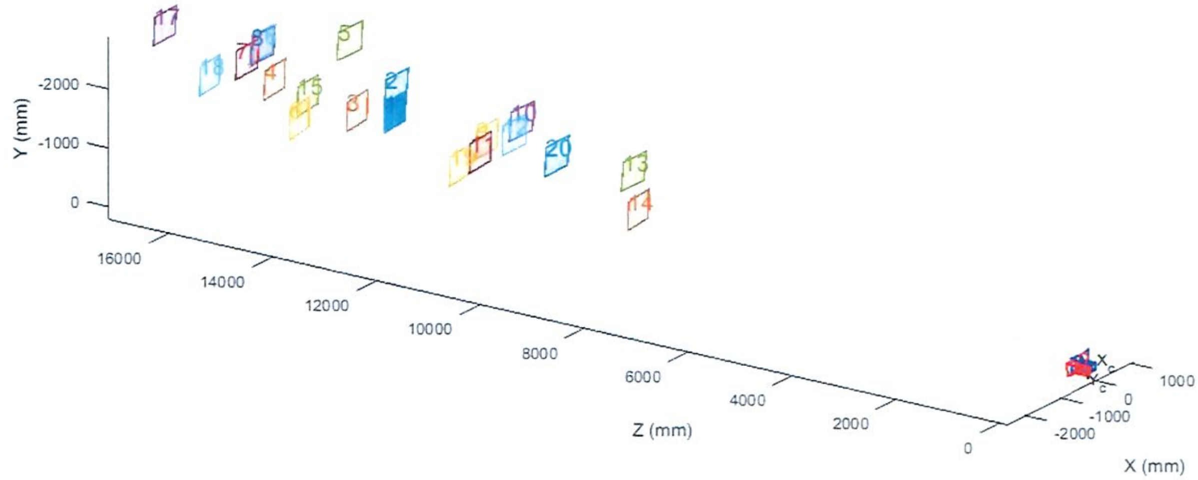

Source – Created by the author

The test evidenced the lack of accuracy of the stereo system developed in this research. By performing multiple field tests with the stereo vision system, it was concluded that the method was not appropriated for the objectives of this research. Although stereo systems are efficient in machine vision applications, the available resources for this research are not suitable to build a precise stereo system. Firstly, the used optical lenses have a narrow viewing angle. For precision applications in machine vision, lenses with wide viewing angle are usually used. A wide viewing angle certifies a higher quality disparity map. Second, the correspondence process of stereo images is a complicated task. The improper image matching affects the accuracy of the method.

5.1.2 Pinhole camera method

The errors and the accuracy of the method were calculated up to a distance of 25 meters using the Eq. 23 and 24. The results of accuracy of the method are shown at Table 5.

Table 5 – Accuracy of pinhole camera method at different distances

Distance (m)	Average error			Accuracy	
	X (mm)	Y (mm)	Z (mm)	Planar (%)	Stereo (%)
5	4,20	2,43	1,25	94,58	92,31
10	3,35	1,95	0,52	96,14	94,27
15	2,29	19,04	0,37	97,33	78,88
20	14,29	6,85	0,10	85,63	79,87
25	24,02	20,35	0,13	75,88	61,47

Source – Created by the author

For distances exceeding 25 meters, the average error exceeds the 50 mm. Consequently, the field of operation with high accuracy of the pinhole camera method was 25 meters. Figure 46 shows the location mapping of the visual system in all the images taken to perform the visual accuracy test up until 25 meters.

As shown in this analysis, the accuracy error increased proportionally as the distance from the vision systems to the checkerboard pattern. With the accuracy calculations of the pinhole camera method, it was concluded that the method is effective to map the position of the tractor in the field. The method obtains a maximum error of 24 mm until 25 meters. Therefore, this method was selected to perform the tests development of this research, installing the visual system in the vehicle.

Figure 46 – Location mapping of calibration images for the pinhole camera method until 25 meters

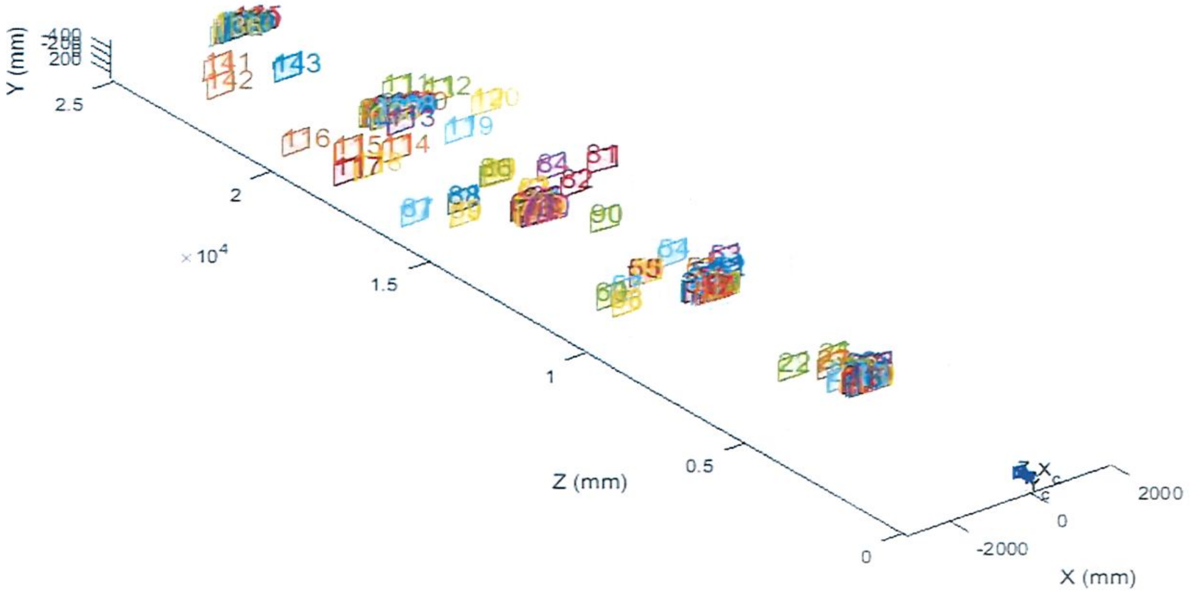

Source – Created by the author

5.2 Mapping of the vehicle's location in field conditions

As mentioned previously, three tests were performed at each speed of operation using the visual system installed in the vehicle. Table 6 shows the number of frames processed in each test by the pinhole camera method. These frames were used to obtain the location of the vehicle in the test field and calculate the auto-guidance system error. The frames captured in the first 5 meters were rejected since the vehicle was not stabilized in the auto-guidance mode during this distance interval. Figure 47 shows the detection of the checkerboard in the test field and its position (0, 0, 0) in the local coordinate system.

Table 6 – Number of frames processed at each operating speed

Speed of operation (km/h)	Number of frames
4.0	1223
4.5	1179
5.0	1099
5.5	905

Source – Created by the author

Figure 47 – Planar checkerboard pattern detection in field test

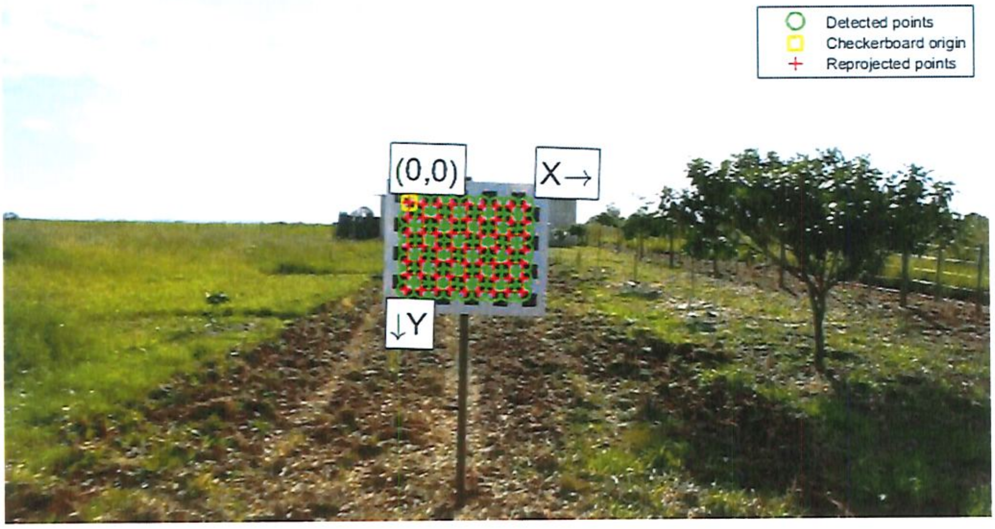
○ Detected points
□ Checkerboard origin
+ Reprojected points
(0,0)
X→
↓Y

Source – Created by the author

Figures 48, 49, 50 and 5 show the tractor location mapping during field tests at speeds of 4.0 km/h, 4.5 km/h, 5.0 km/h and 5.5 km/h respectively. The location of the vehicle was mapped to each vide frame, and then the vehicle's trajectory was constructed by sequentially ordering all video frames. At all operating speeds, the vehicle moves oscillating using the programmed line AB.

Figure 48 – Mapping of tractor trajectory in auto-guidance mode at 4.0 km/h

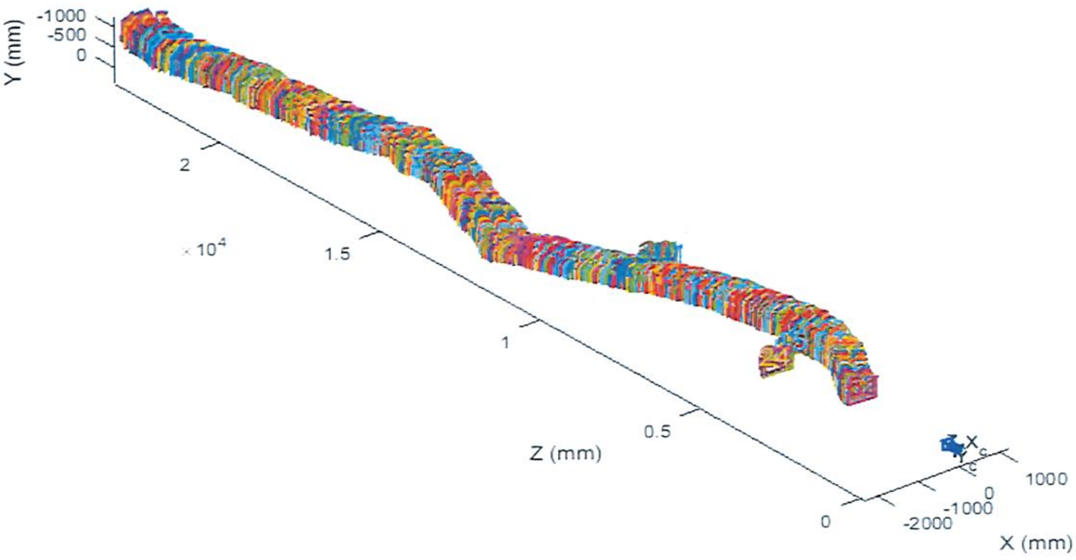

Source – Created by the author

Figure 49 – Mapping of tractor trajectory in auto-guidance mode at 4.5 km/h

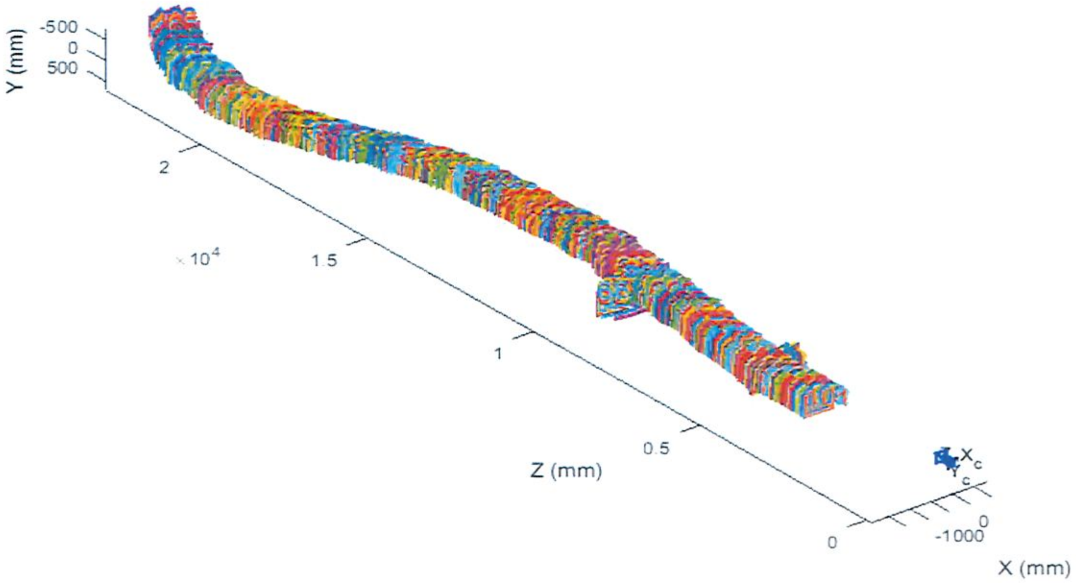

Source – Created by the author

Figure 50 – Mapping of tractor trajectory in auto-guidance mode at 5.0 km/h

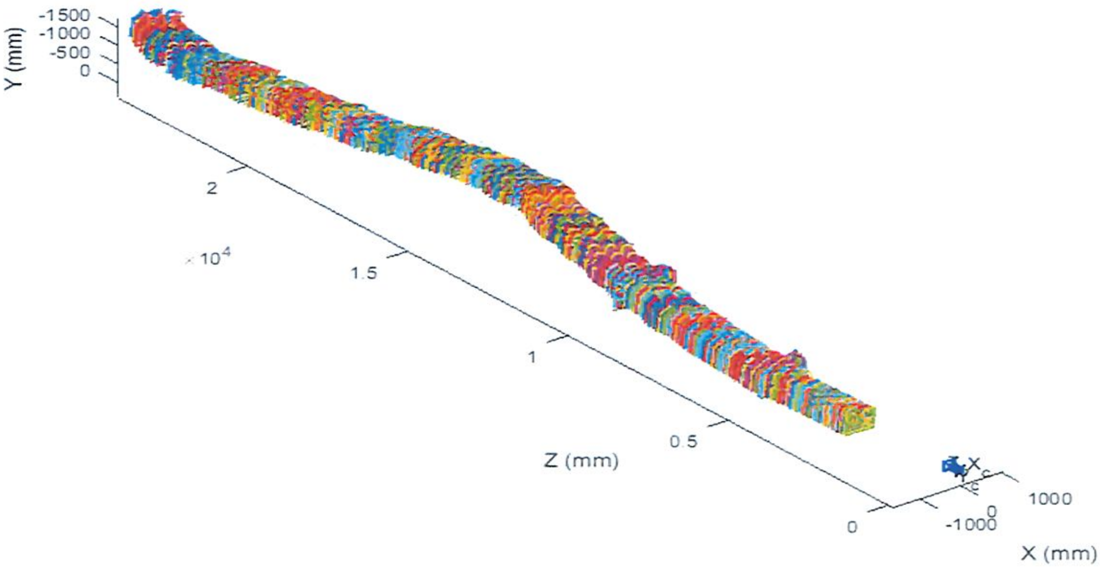

Source – Created by the author

Figure 51 – Mapping of tractor trajectory in auto-guidance mode at 5.5 km/h

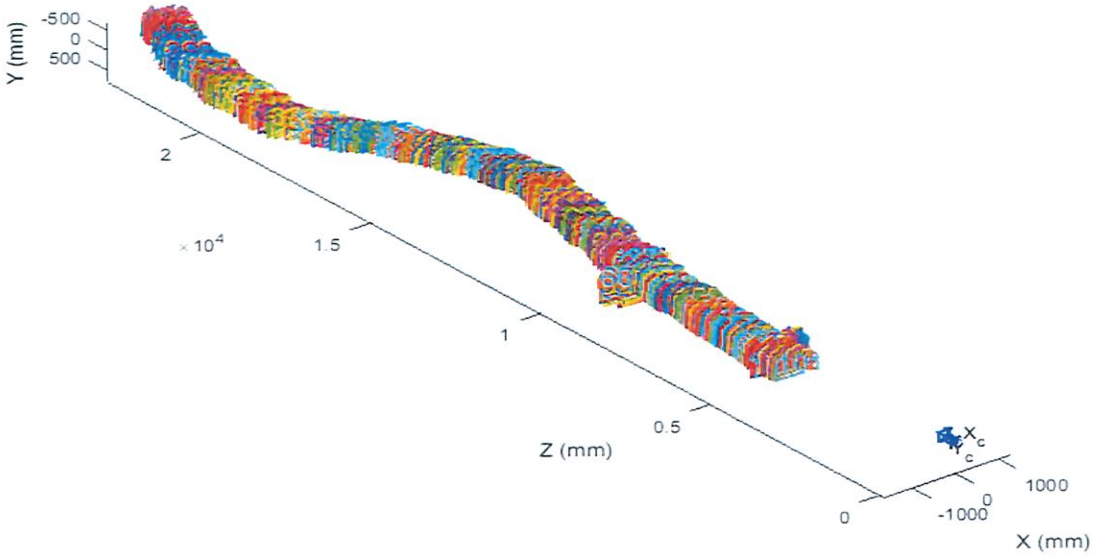

Source – Created by the author

Figures 52, 53, 54, and 55 show the auto-guidance system errors (using Eq. 29) along the path until 25 meters at different operating speeds. In the graphs, it is possible to observe that the tractor made an oscillating movement through the programmed line. As the tractor increased the operating speed the wavelength increased also, which means that the auto-guidance system had greater difficulties to follow the programmed line AB at greater operating speeds. This behavior corroborates with the results reported by Easterly *et al.* (2010) and Harbuck *et al.* (2006).

Figure 52 – Auto-guidance system error at 4.0 km/h

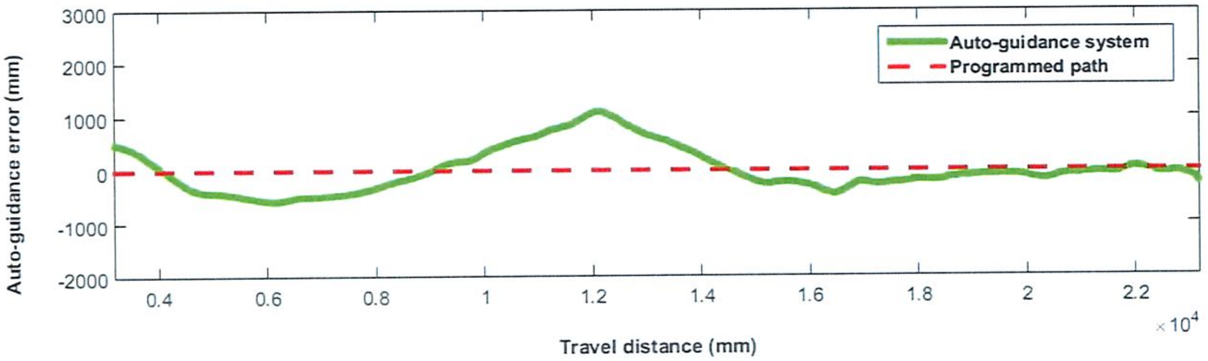

Source – Created by the author

At 4.0 km/h, the tractor movement oscillated through the programmed line with a half wavelength of 5.0 meters. At the end of the path, the vehicle stabilized in the programmed path.

Figure 53 – Auto-guidance system error at 4.5 km/h

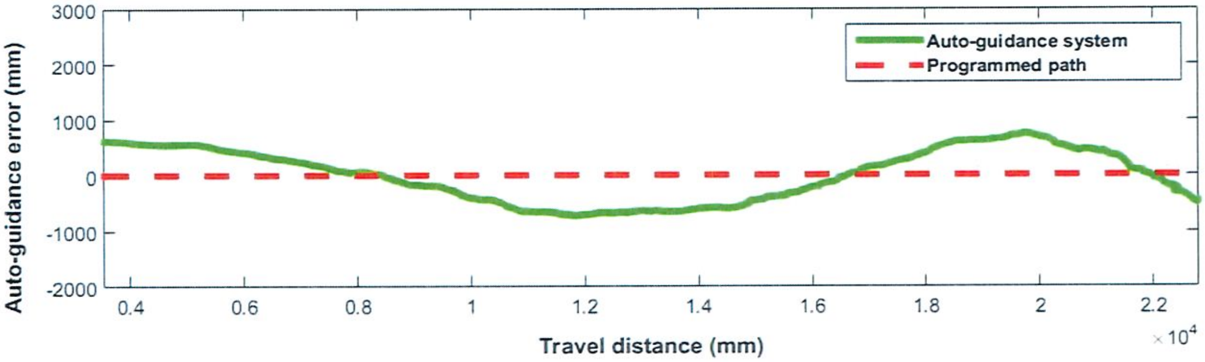

Source – Created by the author

At 4.5 km / h, the tractor kept the oscillatory movement through the programmed line with a half wavelength of 8.5 meters and soft wave peaks in the correction of the auto-guidance system.

Figure 54 – Auto-guidance system error at 5.0 km/h

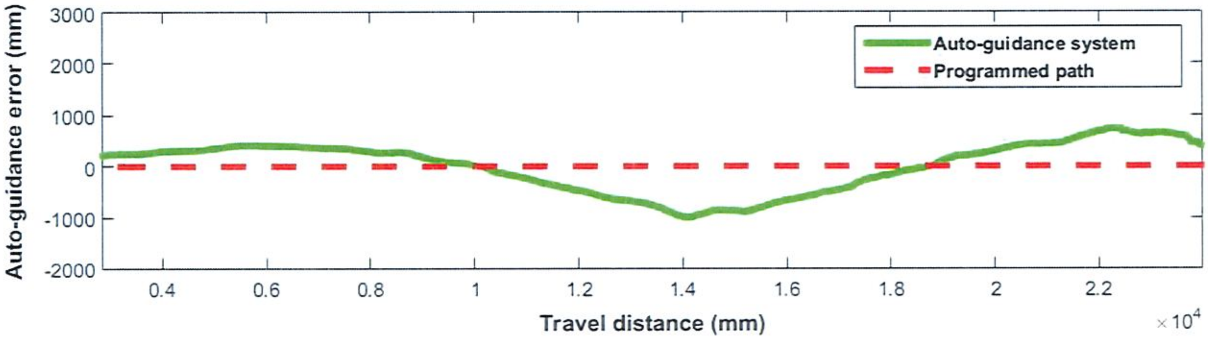

Source – Created by the author

At 5.0 km / h, the tractor kept the oscillatory movement through the programmed line with a half wavelength of 9.0 meters and soft wave peaks in the correction of the auto-guidance system.

At 5.5 km / h, the tractor kept the oscillatory movement through the programmed line with a half wavelength of 8.0 meters but with greater and pronounced wave peaks in the correction of the auto-guidance system.

Figure 55 – Auto-guidance system error at 5.5 km/h

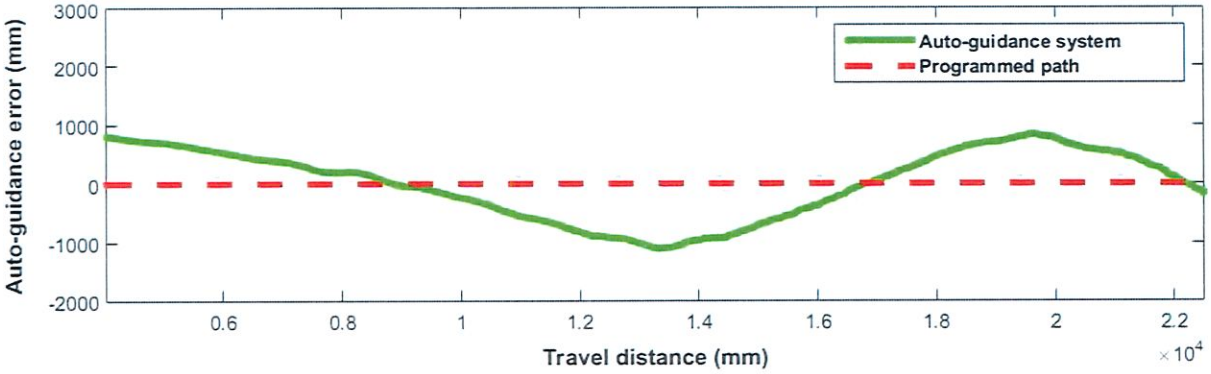

Source – Created by the author

There is a 5% of frames seriously affected by the vibration of the vehicle, generating lack of quality and a wrong calculation of the vehicle localization, therefore, this percentage of frames was discarded. Table 7 summarizes the auto-guidance system errors at different operating speeds. The table shows the auto-guidance system errors for the specific field conditions on the field at LANAPRE – Embrapa Instrumentation São Carlos. The standard deviation and the maximum error were also calculated. The maximum error is defined as the maximum error calculated by 95% of the frames processed.

Table 7 – Auto-guidance system errors

Speed of operation (km/h)	Average error (mm)	Standard deviation (mm)	Maximum error (mm)
4.0	332	214	653
4.5	349	206	727
5.0	447	271	886
5.5	462	256	942

Source – Created by the author

Table 7 shows that the auto-guidance system accuracy decreases at higher operating velocities. This behavior is in accordance to the literature. Neverthless, the accuracy of the system is also affected by the conditions and characteristics of the test terrain at LANAPRE – Embrapa Instrumentation São Carlos. For this reason, it is necessary to test the auto-guidance system on a paved surface where the soil conditions do not affect the accuracy of the system.

5.3 Validation of the proposed methodology

This section presents the results of comparison between the method developed in this research and the methodology developed by Easterly *et al.* (2010) on a paved surface. Table 8 shows the number of frames processed at each test using the validation methodology in the different speeds of operation.

Table 8 – Number of frames processed using the validation methodology

Speed of operation (km/h)	Number of frames
4.0	1820
4.5	1674
5.0	1455
5.5	1376

Source – Created by the author

In the evaluation methodology, a percentage of frames are also discarded because are affected by the vibration of the vehicle, which generate erratic calculations of the vehicle location. Those discarded frames reach a percentage of 5% of the total frames in each test. Table 9 shows the auto-guidance system errors using the validation methodology proposed by Easterly *et al.* (2010).

Table 9 – Auto-guidance system errors using the validation methodology

Speed of operation (km/h)	Average error (mm)	Standard deviation (mm)	Maximum error (mm)
4.0	71	39	128
4.5	73	48	163
5.0	75	53	177
5.5	64	40	148

Source – Created by the author

As expected, the auto-guidance system error increased as the operating speed of the vehicle increased. However, with values lower than obtained on the ground surface since it is possible to minimize the errors caused by the conditions of the terrain.

Using the same trajectory, the computational vision using the pinhole camera method was tested to calculate the errors of the auto-guidance system on the paved surface. The pinhole camera method was only tested at a distance of 25 meters towards the checkerboard pattern. The results obtained by the pinhole camera method are shown in Table 10.

Table 10 – Auto-guidance system errors using the pinhole camera method on flat surface

Speed of operation (km/h)	Average error (mm)	Standard deviation (mm)	Maximum error (mm)
4.0	74	41	159
4.5	85	47	182
5.0	94	53	197
5.5	84	43	160

Source – Created by the author

The error values calculated by the pinhole camera method were slightly higher than obtained by the validation methodology developed by Easterly *et al.* (2010). The comparison between the validation methodology and the pinhole camera method developed in this research is shown in the Table 11.

Table 11 – Auto-guidance system errors using validation methodology vs pinhole camera method

Speed of operation (km/h)	Error by validation methodology (mm)	Error by pinhole camera method (mm)
4.0	71	74
4.5	73	85
5.0	75	94
5.5	64	84

Source – Created by the author

It can be noted that the average errors values by both methodologies had a constant growth as the operating speed increased. The results shown in table 11 prove that the auto-guidance system complies with the manufacturer's specifications, which specifies that the system error is under 100 mm. The graphs in Figures 56, 57, 58, and 59 show the cumulative errors distribution for both methodologies at operating speeds of 4.0 km/h, 4.5 km/h, 5.0 km/h, and 5.5 km/h respectively.

Figure 56 – Auto-guidance system errors, validation method vs pinhole camera method (4.0 km/h)

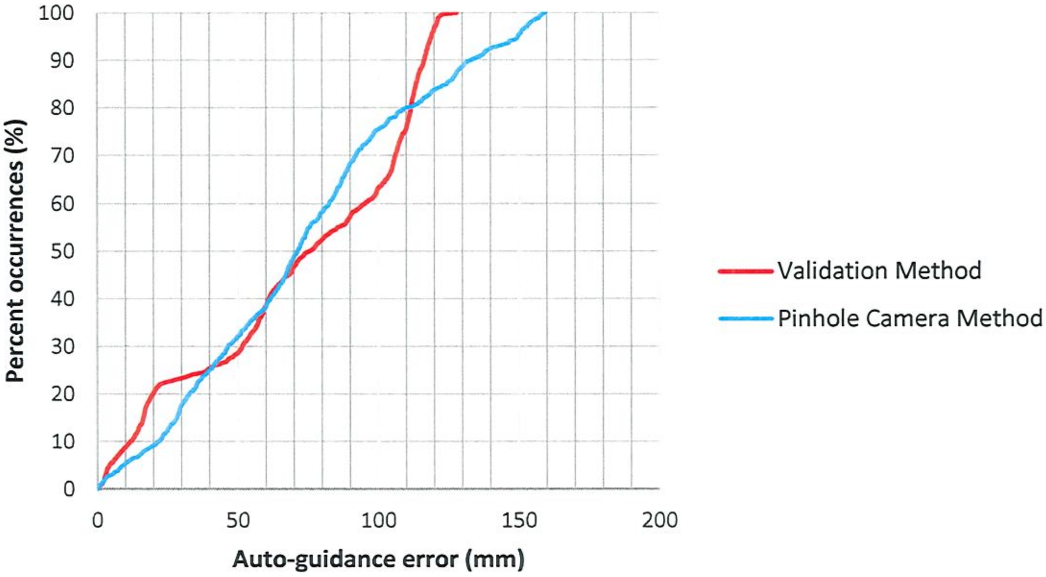

Source – Created by the author

Figure 57 – Auto-guidance system errors, validation method vs pinhole camera method (4.5 km/h)

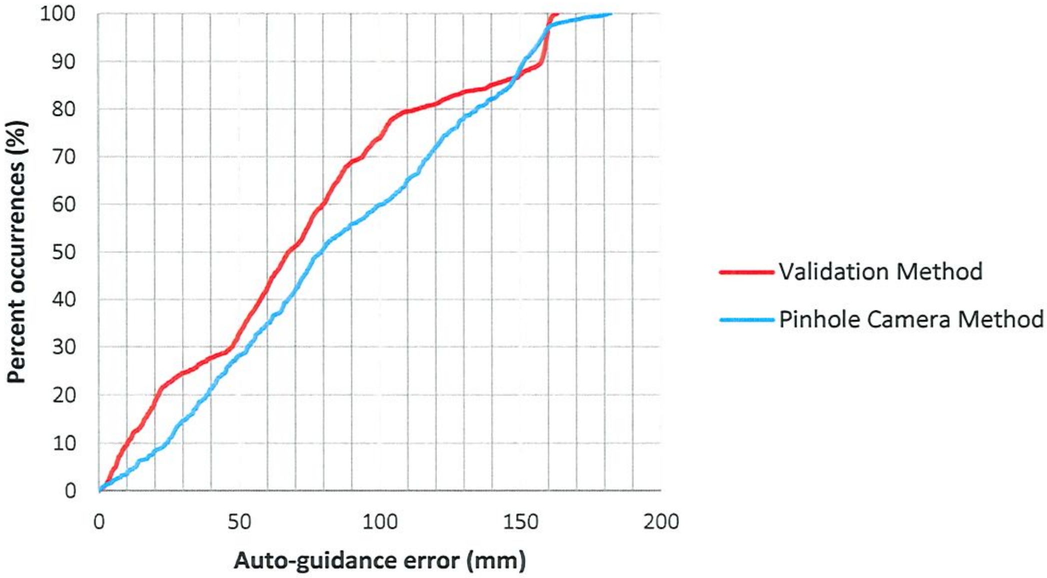

Source – Created by the author

Figure 58 – Auto-guidance system errors, validation method vs pinhole camera method (5.0 km/h)

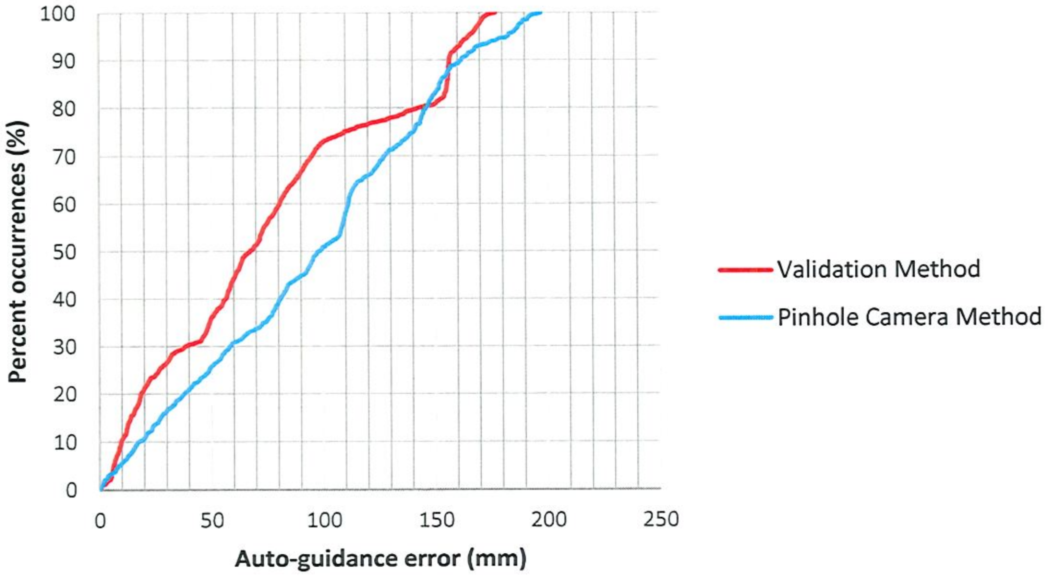

Source – Created by the author

Figure 59 – Auto-guidance system errors, validation method vs pinhole camera method (5.5 km/h)

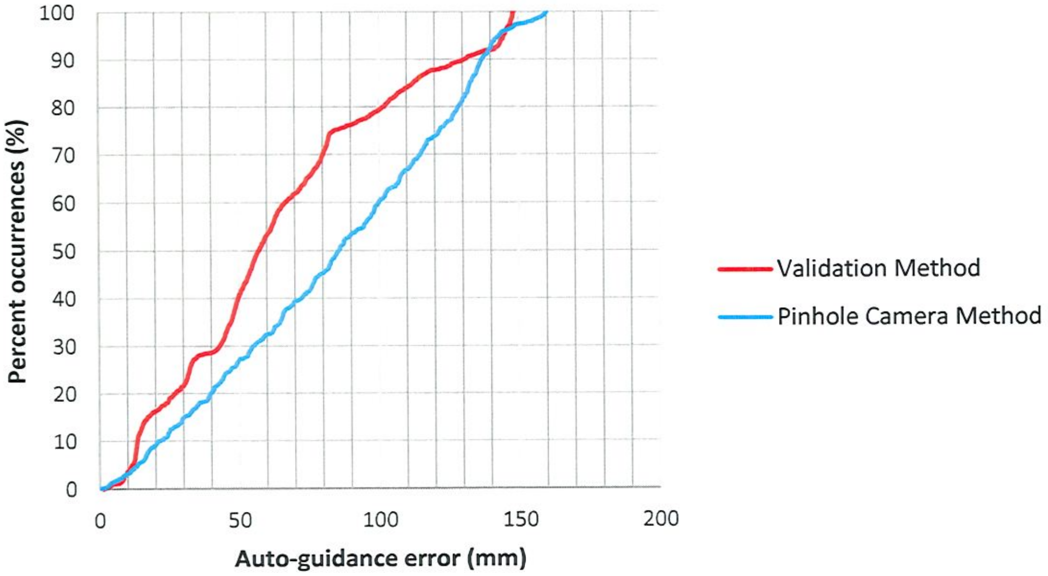

Source – Created by the author

For both methodologies, the auto-guidance system error values presented a constant distribution. In these results, it can be observed that the results extracted by using the methodology developed in this work had a significant correlation with the results obtained by using the validation methodology. With the exception of the test performed at 4 km/h, the validation methodology presents results slightly higher than the results obtained by the methodology developed in this research. However, both methodologies do not differ more than

20 mm in their results. This indicates that the accuracy of the proposed methodology in this research can reach 24 mm, as was shown in Section 5.1.2.

6 CONCLUSIONS

The use of computer vision method can be an alternative to evaluate the accuracy of the auto-guidance system under real field conditions. However, the selection of the appropriate instrumentation parameters to achieve high accuracy is an important challenge.

The stereo vision method is widely used in the mapping of trajectory of a vehicle at outdoor environment. However, in this research, the method reached low levels of accuracy due the design constraints. The precision of the stereo vision method is affected by the complexity of the construction using two single cameras. Another factor that influences the accuracy of the stereo vision method is the complex process of defining its parameters as the focal lens of cameras, the baseline and the alignment between cameras.

The computational vision using the pinhole camera method proved to be highly accurate being capable of calculating the tractor location at millimeter accuracy level. This method made possible the accuracy evaluation of the auto-guidance system implemented in the tractor under real field conditions. An important point to consider is that 5% of the frames processed have low quality because they are affected by the vibration of the vehicle caused by the dynamics of the vehicle in the field, those frames are rejected to improve the accuracy of the visual system. The approach developed in this research reaches an accuracy of 24 mm until 25 meters to the checkerboard, for smaller distances the accuracy increases considerably.

The average errors of the auto-guidance system in the field tests were 332 mm, 349 mm, 447 mm, and 462 mm at speeds of 4.0 km/h, 4.5 km/h, 5.0 km/h, and 5.5 km/h respectively. The maximum auto-guidance system error is defined in this research as the maximum error perceived by 95% of the errors calculated by the pinhole camera method. Therefore, the maximum errors of the auto-guidance system were 653 mm, 727 mm, 886 mm, and 942 mm at speeds of 4.0 km/h, 4.5 km/h, 5.0 km/h, and 5.5 km/h respectively. It is highlighted that these errors were the auto-guidance system errors for the specific terrain condition in the field tests developed in this research.

The methodology proposed in this research was validated by the methodology developed by Easterly *et al.* (2010). The results were satisfactory, obtaining a remarkable correspondence in the data obtained by both methods in all tests performed. With the validation test, it was concluded that the proposed methodology is highly accurate and reliable to evaluate auto-guidance systems under real field conditions.

With the tests carried out on the paved surface it was possible to prove that the auto-guidance system is highly accurate, the error of the auto-guidance system complies with the specifications given by the manufacturer (under 100 mm). The auto-guidance system error rates are considerably low, considering the tractor and the auto-guidance system implemented reliable for automated agricultural operations.

6.1 Future perspectives

The developed approach can be applicable to real field conditions being robust to errors due to geographic positioning GPS errors, low data acquisition rate, vehicle dynamics and field environment (slopes, soil condition, etc.). Despite having these advantages, the approach also has certain restrictions. The main restriction is the short test field that reaches only 25 meters. That distance was selected since the frames taken after 25 meters respect to the checkerboard pattern were distorted due to the vibration of the tractor. In addition, 5% of the processed frames have low quality since they are affected by the vibration of the vehicle caused by the dynamics of the vehicle in the field. A possible solution for both problems is the use of optical lens of wide focal length and an image stabilizer. This solution may improve the method by increasing the test distance and by improving the precision of calibration of the camera parameters.

BIBLIOGRAPHIC REFERENCES

ADAMCHUK, V. I.; HOY, R. M.; MEYER, G. E.; KOCHER, M. F. GPS-based autoguidance test program development. **Precision agriculture**, v. 7, n. 3-6, 2007.

BALASTREIRE, L. A. **O estado da arte da agricultura de precisão no Brasil**. Piracicaba: [s.n.], 2000.

BLANC-TALON, J.; PHILIPS, W.; POPESCU, D. **Advanced Concepts for Intelligent Vision Systems:** 11th International Conference, ACIVS 2009 Bordeaux, France, September 28--October 2, 2009 Proceedings. [S.l.]: Springer Science & Business Media, 2009.

BODKIN, B. H. Real-Time Mobile Stereo Vision, 2012.

BOUGUET, J. Y. Camera Calibration Toolbox for Matlab, 2004. Available in: <http://www.vision.caltech.edu/bouguetj/calib_doc/>. Access in: 13 July 2016.

BOUGUET, J. Y. Camera calibration toolbox for Matlab, 2004.

BRANDÃO, Z. N.; BEZERRA, M. V. C.; FREIRE, E. C.; DA SILVA, B. B. Agricultura de precisão para gerenciamento do algodão. **O Agronegócio do Algodão no Brasil**, v. 20, 2008.

BROX, T.; BRUHN, A.; PAPENBERG, N.; WEICKERT, J. High accuracy optical flow estimation based on a theory for warping. **Computer Vision-ECCV 2004**, p. 25-36, 2004.

CAMPOS, A. C.; MENDOÇA, J.; VILELA DE RESENDE, A.; BASSOI, L. H.; INAMASU, R. **Agricultura de Precisão:** Resultados de um Novo Olhar. Brasilia, DF: Editorial Cubo, 2014. 596 p.

CHEN, T. W.; CHEN, Y. L.; CHIEN, S. Y. **Fast image segmentation based on K-Means clustering with histograms in HSV color space**. Multimedia Signal Processing, 2008 IEEE 10th Workshop on. Shangri-La Hotel Cairns, Australia: IEEE. 2008. p. 322-325.

CHERUBINI, A.; GRECHANICHENKO, B.; SPINDLER, F.; CHAUMETTE, F. **Avoiding Moving Obstacles during Visual Navigation**. Robotics and Automation (ICRA), 2013 IEEE International Conference on. [S.l.]: IEEE. 2013. p. 3069-3074.

CHON, J. H.; PARK, Y. W.; SONG, J. B.; K-WEON, I. S. Localization using GPS and VISION aided INS with an image database and a network of a ground-based reference station in outdoor environments. **International Journal of Control, Automation and Systems**, p. 716-725, 2011.

CONTRIBUTORS, W. Decimal degrees. **Wikipedia, The Free Encyclopedia.**, 2017. Available in: <https://en.wikipedia.org/w/index.php?title=Decimal_degrees&oldid=791469325>. Access in: 3 March 2017.

CONTRIBUTORS, W. Real Time Kinematic. **Wikipedia, The Free Encyclopedia.**, 2017. Available in: <https://en.wikipedia.org/w/index.php?title=Real_Time_Kinematic&oldid=791117090>. Access in: 12 July 2017.

CUI, P. Y.; XU, T. L. **Data fusion algorithm for INS/GPS/Odometer navigation system**. Proc. of IEEE Conf. Industrial Electronics and Applications. [S.l.]: [s.n.]. 2007. p. 1893-1897.

DAL MUTTO, C.; ZANUTTIGH, P.; CORTELAZZO, G. M.; MATTOCCIA, S. Scene segmentation assisted by stereo vision. **CURRENT ADVANCEMENTS IN STEREO VISION**, p. 23, 2012.

DALAL, N.; TRIGGS, B. **Histograms of oriented gradients for human detection**. Computer Vision and Pattern Recognition, 2005. CVPR 2005. IEEE Computer Society Conference on. [S.l.]: IEEE. 2005. p. 886-893.

EASTERLY, D. R.; ADAMCHUK, V. I.; KOCHER, M. F.; HOY, R. M. Using a vision sensor system for performance testing of satellite-based tractor auto-guidance. **Computers and Electronics in Agriculture**, v. 72, n. 2, p. 107-118, 2010.

EASTERLY, D. R.; ADAMCHUCK, V. **Auto-guidance error measurement using a visual sensor**. ASABE Annual Meeting Paper. [S.l.]: [s.n.]. 2008.

FANTO, P. L. **Automatic Positioning and Design of a Variable Baseline Stereo Boom**. [S.l.]: University Libraries, Virginia Polytechnic Institute and State University, 2012.

FETÍC, A.; JURÍC, D.; OSMANKOVÍC, D. **The procedure of a camera calibration using Camera Calibration Toolbox for MATLAB**. MIPRO, 2012 Proceedings of the 35th International Convention. [S.l.]: IEEE. 2012. p. 1752-1757.

GALLUP, D.; FRAHM, J. M.; MORDOHAI, P.; POLLEFEYS, M. **Variable baseline/resolution stereo**. Computer Vision and Pattern Recognition, 2008. CVPR 2008. IEEE Conference on. [S.l.]: IEEE. 2008. p. 1-8.

GAN-MOR, S.; CLARK, R. L.; UPCHURCH, B. L. Implement lateral position accuracy under RTK-GPS tractor guidance. **Computers and Electronics in Agriculture**, 2007. 31-38.

GAN-MOR, S.; CLARK, R. L.; UPCHURCH, B. L. Implement lateral position accuracy under RTK-GPS tractor guidance. **Computers and Electronics in Agriculture**, v. 59, n. 1, p. 31-38, 2007.

GARCIA-FAVROT, O.; PARENT, M. **Laser scanner based slam in real road and traffic environment**. IEEE International Conference Robotics and Automation (ICRA09). Workshop on Safe navigation in open and dynamic environments Application to autonomous vehicles. [S.l.]: [s.n.]. 2009.

GOMEZ-GIL, J.; ALONSO-GARCIA, S.; GÓMEZ-GIL, F. J.; STOMBAUGH, T. A simple method to improve autonomous GPS positioning for tractors. **Sensors**, p. 5630-5644, 2011.

GONZALEZ, R. C.; WOODS, R. E. **Digital Image Processing**. [S.l.]: Pearson/Prentice Hall, 2008.

GUIJARRO, M.; PAJARES, G.; RIOMOROS, I.; HERRERA, P. J.; BURGOS-ARTIZZU, X.P.; RIBEIRO, A. Automatic segmentation of relevant textures in agricultural images. **Computers and Electronics in Agriculture**, p. 75-83, 2011.

HAAR, A. Zur theorie der orthogonalen funktionensysteme. **Mathematische Annalen**, p. 331-371, 1910.

HARBUCK, T. L.; FULTON, J. P.; MCDONALD, T. P.; BRODBECK, C. J. Evaluation of GPS autoguidance systems over varying time periods. **ASABE Paper**, n. 061042, 2006.

HARRIS, C.; STEPHENS, M. **A combined corner and edge detector**. Alvey vision conference. [S.l.]: Citeseer. 1988. p. 10.5244.

HARTLEY, R.; ZISSERMAN, A. **Multiple view geometry in computer vision**. [S.l.]: Cambridge university press, 2003.

HEIKKILA, J.; SILVEN, O. **A four-step camera calibration procedure with implicit image correction**. Computer Vision and Pattern Recognition, 1997. Proceedings., 1997 IEEE Computer Society Conference on. [S.l.]: IEEE. 1997. p. 1106-1112.

KISE, M.; ZHANG, Q.; ROVIRA-MÁS, F. A Stereovision-based Crop Row Detection Method for Tractor-automated Guidance. **Biosystems Engineering**, p. 357-367, 2005.

KONOLIGE, K.; AGRAWAL, M.; SOLA, J. Large-scale visual odometry for rough terrain. In: **Robotics research**. [S.l.]: Springer, 2010. p. 201-212.

LADYS LAW SKARBEK, W.; KOSCHAN, A. Colour image segmentation a survey. **IEEE Transactions on circuits ands ystems for Video Technology**, 1994.

LARSEN, W.; NIELSEN, G.; TYLER, D. Precision navigation with GPS. **Computers and Electronics in Agriculture**, p. 85-95, 1994.

LIM, Y. C.; LEE, C. H.; KWON, S.; JUNG, W. Y. **Distance estimation algorithm for both long and short ranges based on stereo vision system**. Intelligent Vehicles Symposium, 2008 IEEE. [S.l.]: IEEE. 2008. p. 841-846.

LIN, C. C. **Detecting and tracking moving objects from a moving platform**. [S.l.]: Georgia Institute of Technology, 2012.

LIU, B.; ADAMS, M.; IBANEZ-GUZMAN, J. **Multi-aided inertial navigation for ground vehicles in outdoor uneven environments**. Robotics and Automation, 2005. ICRA 2005. Proceedings of the 2005 IEEE International Conference on. [S.l.]: IEEE. 2005. p. 4703-4708.

LOWE, D. G. Distinctive Image Features From Scale-Invariant Keypoints. **International journal of computer vision**, p. 91-110, 2004.

MACHADO, T. M.; MOLIN, J. P.; POVH, F. P.; SALVI, J. V. Metodologia para avaliação do desempenho de receptor de GPS de uso agrícola em condição cinemática. **Engenharia Agrícola**, p. 121-129, 2010.

MATHWORKS. www.mathworks.com, 1994. Available in: <https://www.mathworks.com/help/vision/ug/camera-calibration.html?searchHighlight=pinhole%20camera&s_tid=doc_srchtitle>. Access in: 3 February 2017.

MATTOCCIA, S. Stereo Vision: Algorithms and applications. **University of Bologna**, Bologna, Italia, 2011.

MEGURO, J. I.; AMANO, Y.; HASHIZUME, T.; TAKIGUCHI, J.I. **Omni-directional Motion Stereo Vision based on Accurate GPS/INS Navigation System**. Proceedings of the 2nd Workshop on Integration of Vision and Inertial Sensors. [S.l.]: [s.n.]. 2005.

MINISTERIO DA AGRICULTURA, PECUÁRIA E ABASTECIMENTO. **Agricultura de Precisão/Boletin Tecnico**. Brasilia, DF. 2009.

MITCHELL, J. The application of inertial navigation technology in land vehicles. **Journal of navigation**, p. 81-87, 1995.

NAJJAR, E.; BONNIFAIT, P. A road-matching method for precise vehicle localization using belief theory and kalman filtering. **Autonomous Robots**, p. 173-191, 2005.

OLLIS, M.; STENTZ, A. **First results in vision-based crop line tracking**. Robotics and Automation, 1996. Proceedings., 1996 IEEE International Conference on. [S.l.]: IEEE. 1996. p. 951-957.

PEREZ-RUIZ, MANUEL.; SLAUGHTER, D. C.; GLIEVER, C.; UPADHYAYA, S. K. Tractor-based Real-time Kinematic-Global Positioning System (RTK-GPS) guidance system for geospatial mapping of row crop transplant. **Biosystems engineering**, v. 111, n. 1, p. 64-71, 2012.

PEYRET, F.; BETAILLE, D.; HINTZY, G. High-precision application of GPS in the field of real-time equipment positioning. **Automation in Construction**, p. 299-314, 2000.

REID, J. F. **Precision guidance of agricultural vehicles**. SME Meeting, Sapporo, Japan. UILU-ENG-7031. [S.l.]: [s.n.]. 1998.

ROSTEN, E.; DRUMMOND, T. **Fusing points and lines for high performance tracking**. Computer Vision, 2005. ICCV 2005. Tenth IEEE International Conference on. [S.l.]: IEEE. 2005. p. 1508-1515.

ROVIRA-MÁS, F.; ZHANG, Q.; REID, J. F.; WILL, J. D. Hough-transform-based vision algorithm for crop row detection of an automated agricultural vehicle. **Proceedings of the Institution of Mechanical Engineers, Part D: Journal of Automobile Engineering**, p. 999-1010, 2005.

ROVIRA-MÁS, F.; REID, J. F.; ZHANG, Q. Stereovision data processing with 3D density maps for agricultural vehicles. **Transactions of the ASABE**, p. 1213-1222, 2006.

ROVIRA-MÁS, F.; WANG, Q.; ZHANG, Q. **Configuration of Stereo Systems for Off-road**. Proceedings of the American Society of Agricultural and Biological Engineers Annual International Meeting (ASABE'08). [S.l.]: ASABE. 2008.

ROVIRA-MÁS, F.; WANG, Q.; ZHANG, Q. Bifocal stereoscopic vision for intelligent vehicles. **International journal of vehicular technology**, 2009.

ROVIRA-MÁS, F.; ZHANG, Q.; HANSEN, A. C. **Mechatronics and intelligent systems for off-road vehicles**. [S.l.]: Springer London, 2010.

ROYER, E.; LHUILLIER, M.; DHOME, M.; LAVEST, J. M. Monocular vision for mobile robot localization and autonomous navigation. **International Journal of Computer Vision**, v. 74, n. 3, p. 237-260, 2007.

RUSS, J. C. **The Image Processing Handbook, Sixth Edition**. [S.l.]: CRC Press, 2016.

SÁNCHEZ, T.; AUGUSTO, A. **Image Space and Time Interpolation for Video Navigation**. [S.l.]. 2011.

SCHETTINI, R. A segmentation algorithm for color images. **Pattern Recognition Letters**, p. 499-506, 1993.

STOLL, A.; DIETER KUTZBACH, H. Guidance of a Forage Harvester with GPS. **Precision Agriculture**, p. 281–291, 2000.

SURAL, S.; QIAN, G.; PRAMANIK, S. **Segmentation and histogram generation using the HSV color space for image retrieval**. Image Processing. 2002. Proceedings. 2002 International Conference on. [S.l.]: IEEE. 2002. p. II-II.

TUOHY, S.; O'CUALAIN, D.; JONES, E.; GLAVIN, M. **Distance determination for an automobile environment using inverse perspective mapping in OpenCV**. Signals and Systems Conference (ISSC 2010), IET Irish. [S.l.]: IET. 23 June 2010. p. 100-105.

VIDAL, R.; MA, Y. A unified algebraic approach to 2-D and 3-D motion segmentation. **Computer Vision-ECCV 2004**, p. 1-15, 2004.

VIOLA, P.; J JONES, M. **Rapid object detection using a boosted cascade of simple features**. Computer Vision and Pattern Recognition, 2001. CVPR 2001. Proceedings of the 2001 IEEE Computer Society Conference on. [S.l.]: IEEE. 2001. p. I-I.

Wang, Z.; WU, W.; Xu, X.; Xue, D. Recognition and location of the internal corners of planar checkerboard calibration pattern image. **Applied mathematics and computation**, p. 894–906, 2007.

WEI, L.; CAPELLE, C.; RUICHEK, Y. **Unscented Information Filter Based Multi-sensor Data Fusion Using Stereo Camera, Laser Range Finder and GPS Receiver for Vehicle Localization**. Intelligent Transportation Systems (ITSC), 2011 14th International IEEE Conference on. [S.l.]: IEEE. 2011. p. 1923-1928.

YAHYA, A.; ZOHADIE, M.; KHEIRALLA, A. F.; GIEW, S. K.; BOON, N. E. Mapping system for tractor-implement performance. **Computers and electronics in agriculture**, v. 69, n. 1, p. 2-11, 2009.

YANG, Y. C.; FARRELL, J. A. Magnetometer and differential carrier phase GPS-aided INS for advanced vehicle control. **IEEE transactions on Robotics and Automation**, p. 269-282, 2003.

ZHANG, Z. A flexible new technique for camera calibration. **IEEE Transactions on pattern analysis and machine intelligence**, p. 1330-1334, 2000.

ZHENG, L.; ZHANG, J.; WANG, Q. Mean-shift-based color segmentation of images containing green vegetation. **Computers and Electronics in Agriculture**, p. 93-98, 2009.